PHYSICAL REVIEW D **82,** 054024 (2010)

Vacuum properties of mesons in a linear sigma model with vector mesons and global chiral invariance

Denis Parganlija,[1] Francesco Giacosa,[1] and Dirk H. Rischke[1,2]

[1]*Institute for Theoretical Physics, Johann Wolfgang Goethe University, Max-von-Laue-Straße 1, D–60438 Frankfurt am Main, Germany*

[2]*Frankfurt Institute for Advanced Studies, Ruth-Moufang-Straße 1, D–60438 Frankfurt am Main, Germany*

(Received 26 March 2010; published 22 September 2010)

We present a two-flavor linear sigma model with global chiral symmetry and vector and axial-vector mesons. We calculate $\pi\pi$ scattering lengths and the decay widths of scalar, vector, and axial-vector mesons. It is demonstrated that vector and axial-vector meson degrees of freedom play an important role in these low-energy processes and that a reasonable theoretical description requires globally chirally invariant terms other than the vector-meson mass term. An important question for meson vacuum phenomenology is the quark content of the physical scalar $f_0(600)$ and $a_0(980)$ mesons. We investigate this question by assigning the quark-antiquark σ and a_0 states of our model with these physical mesons. We show via a detailed comparison with experimental data that this scenario can describe all vacuum properties studied here except for the decay width of the σ, which turns out to be too small. We also study the alternative assignment $f_0(1370)$ and $a_0(1450)$ for the scalar mesons. In this case the decay width agrees with the experimental value, but the $\pi\pi$ scattering length a_0^0 is too small. This indicates the necessity to extend our model by additional scalar degrees of freedom.

DOI: 10.1103/PhysRevD.82.054024 PACS numbers: 12.39.Fe, 13.20.Jf, 13.75.Lb

I. INTRODUCTION

The fundamental theory of strong interactions, quantum-chromodynamics (QCD), possesses an exact $SU(3)_c$ local gauge symmetry (the color symmetry) and an approximate global $U(N_f)_R \times U(N_f)_L$ symmetry for N_f massless quark flavors (the chiral symmetry). For sufficiently low temperature and density quarks and gluons are confined into colorless hadrons (i.e., $SU(3)_c$ invariant configurations). Thus, it is the chiral symmetry which predominantly determines hadronic interactions in the low-energy region.

Effective field theories which contain hadrons as degrees of freedom rather than quarks and gluons have been developed along two lines which differ in the way in which chiral symmetry is realized: linear [1] and nonlinear [2]. In the nonlinear realization, the so-called nonlinear sigma model, the scalar states are integrated out, leaving the pseudoscalar states as the only degrees of the freedom. On the other hand, in the linear representation of the symmetry, the so-called linear sigma model, both the scalar and pseudoscalar degrees of freedom are present.

In this work, we consider the linear representation of chiral symmetry. An exactly linearly realized chiral symmetry implies that the QCD eigenstates come in degenerate pairs, the so-called chiral partners. Chiral partners have the same quantum numbers with the exception of parity and G-parity—for example, the scalar states sigma and pion and the vector states ρ and a_1, respectively, are chiral partners. Experimental data in vacuum and at sufficiently low temperatures and densities of matter, however, show that the mass degeneracy is lifted, because the chiral $U(N_f)_R \times U(N_f)_L \equiv U(1)_V \times U(1)_A \times SU(N_f)_V \times SU(N_f)_A$ symmetry is broken in two ways: explicitly and spontaneously.

Because of the $U(1)_A$ anomaly [3], the $U(N_f)_R \times U(N_f)_L$ symmetry is broken explicitly by quantum effects to $U(1)_V \times SU(N_f)_V \times SU(N_f)_A$. In the case of small but nonzero degenerate quark masses, the latter is explicitly broken to $U(N_f)_V$. If the quark masses are not degenerate, the $U(N_f)_V$ symmetry is furthermore explicitly broken to $U(1)_V$, corresponding to baryon number conservation. QCD also possesses discrete symmetries such as the charge conjugation (C), parity (P) and time reversal (T) symmetry (CPT), which are to a very good precision separately conserved by strong interactions. This fact offers further constraints in the construction of effective models of QCD. [A review of a possible, although small, CP violation in strong interactions may be found, e.g., in Ref. [4].]

In addition to the explicit breaking of axial symmetry $SU(N_f)_A$ due to nonzero quark masses, the latter symmetry is also spontaneously broken in vacuum by the nonvanishing expectation value of the quark condensate: $\langle \bar{q}q \rangle = \langle \bar{q}_R q_L + \bar{q}_L q_R \rangle \neq 0$ [5]. This symmetry breaking mechanism leads to the emergence of $N_f^2 - 1$ pseudoscalar Goldstone bosons, as well as of massive scalar states representing the chiral partners of the Goldstone bosons. For $N_f = 2$, the three lightest mesonic states, the pions, are identified with these Goldstone bosons of QCD. Their nonvanishing mass arises due to the explicit breaking of the chiral symmetry, rendering them pseudo-Goldstone bosons.

In this paper we study an $N_f = 2$ linear sigma model which contains scalar $(\sigma, \vec{a}_0)$ and pseudoscalar $(\eta, \vec{\pi})$, and in addition also vector $(\omega, \vec{\rho})$ and axial-vector $(f_1, \vec{a}_1)$ degrees of freedom. Usually, such models are constructed under the requirement of local chiral invariance

$U(N_f)_R \times U(N_f)_L$, with the exception of the vector-meson mass term which renders the local symmetry a global one [6,7]. In a slight abuse of terminology, we will refer to these models as locally chirally invariant models in the following. A study of the QCD phase transition and its critical temperature T_c within such a model can be found, e.g., in Ref. [8].

However, as shown in Refs. [6,7,9–11], the locally invariant linear sigma model fails to simultaneously describe meson decay widths and pion-pion scattering lengths in vacuum. As outlined in Ref. [10], there are at least two ways to solve this issue. One way is to utilize a model in which the (up to the vector-meson mass term) local invariance of the theory is retained while higher-order terms are added to the Lagrangian [6,7,9]. The second way which is pursued here is the following: we construct a linear sigma model with global chiral invariance containing all terms up to naive scaling dimension four [12]. The global invariance allows for additional terms to appear in our Lagrangian in comparison to the locally invariant case presented, e.g., in Ref. [8]. We remark that, introducing a dilaton field, one can argue [13,14] that chirally invariant terms of higher order than scaling dimension four should be absent.

In Ref. [11], we have presented a first study of meson decays and pion-pion scattering lengths in vacuum in the framework of the globally invariant linear sigma model. We have distinguished two different assignments for the scalar fields $\sigma = \frac{1}{\sqrt{2}}(\bar{u}u + \bar{d}d)$ and $a_0^0 = \frac{1}{\sqrt{2}}(\bar{u}u - \bar{d}d)$: (i) they may be identified with $f_0(600)$ and $a_0(980)$ which are members of a nonet that in addition consists of $f_0(980)$ and $\kappa(800)$; (ii) they may be identified with $f_0(1370)$ and $a_0(1450)$ which are members of a decuplet that in addition consists of $f_0(1500)$, $f_0(1710)$, and $K_0(1430)$, where the additional scalar-isoscalar state emerges from the admixture of a glueball field [15]. In the following, we will refer to assignment (i) as Scenario I, and to assignment (ii) as Scenario II. In the latter, scalar mesons below 1 GeV are not (predominantly) quark-antiquark states. Their spectroscopic wave functions might contain a dominant tetraquark or mesonic molecular contribution [16]. The correct assignment of the scalar quark-antiquark fields of the model to physical resonances is not only important as a contribution to the ongoing debate about the nature of these resonances, but it is also vital for a study of the properties of hadrons at nonzero temperature and density, where the chiral partner of the pion plays a crucial role [17].

It is important to stress that the theoretical σ and a_0 fields entering the linear sigma model describe pure quark-antiquark states, just as all the other fields (η, $\vec{\pi}$, ω, $\vec{\rho}$, f_1, $\vec{a}_1$). This property can be easily proven by using well-known large-N_c results [18]: the mass and the decay widths of both σ and a_0 fields scale in the model as N_c^0 and N_c^{-1}, respectively.

In this paper we first investigate the consequences of Scenario I on various decay widths and pion-pion scattering lengths. This assignment is disfavored because a consistent description of all experimental data cannot be achieved. To reach this conclusion, vector and axial-vector degrees of freedoms play an important role. On the one hand, their decays (such as $\rho \to \pi\pi$ and $a_1 \to \pi\gamma$) and the role of the ρ meson in $\pi\pi$ scattering provide strong constraints, on the other hand they affect, indirectly but sizably, some decay channels, such as $\sigma \to \pi\pi$. We then present a study of Scenario II. Although the latter is not yet conclusive because additional scalar fields (glueball, tetraquark) are not yet taken into account, our preliminary results for the decay widths (albeit not for the scattering length a_0^0) are consistent with the data.

The paper is organized as follows: in Sec. II, we present the Lagrangian of our model and discuss the parameters which are known to very good precision and thus do not enter the fit of the decay widths and the scattering lengths. In Sec. III, we present the formulas for the decay widths and the pion-pion scattering lengths which will be used to fit the remaining parameters and to compare the results to experimental data. This fit and comparison are discussed in Sec. IV, both for Scenario I and Scenario II. In Sec. V we summarize our results in the conclusions and give an outlook to future work. In the Appendix, we show the explicit form of our Lagrangian in terms of the meson fields.

II. THE LINEAR SIGMA MODEL WITH GLOBAL CHIRAL SYMMETRY

A. The Lagrangian

The Lagrangian of the globally invariant linear sigma model with $U(2)_R \times U(2)_L$ symmetry for $N_f = 2$ reads [6,7,11,19]:

$$\begin{aligned}
\mathcal{L} &= \mathrm{Tr}[(D^\mu\Phi)^\dagger(D^\mu\Phi)] - m_0^2\,\mathrm{Tr}(\Phi^\dagger\Phi) - \lambda_1[\mathrm{Tr}(\Phi^\dagger\Phi)]^2 - \lambda_2\,\mathrm{Tr}(\Phi^\dagger\Phi)^2 - \frac{1}{4}\mathrm{Tr}[(L^{\mu\nu})^2 + (R^{\mu\nu})^2] \\
&+ \frac{m_1^2}{2}\mathrm{Tr}[(L^\mu)^2 + (R^\mu)^2] + \mathrm{Tr}[H(\Phi + \Phi^\dagger)] + c(\det\Phi + \det\Phi^\dagger) - 2ig_2(\mathrm{Tr}\{L_{\mu\nu}[L^\mu, L^\nu]\} + \mathrm{Tr}\{R_{\mu\nu}[R^\mu, R^\nu]\}) \\
&- 2g_3[\mathrm{Tr}(\{\partial_\mu L_\nu - ieA_\mu[t^3, L_\nu] + \partial_\nu L_\mu - ieA_\nu[t^3, L_\mu]\}\{L^\mu, L^\nu\}) + \mathrm{Tr}(\{\partial_\mu R_\nu - ieA_\mu[t^3, R_\nu] + \partial_\nu R_\mu \\
&- ieA_\nu[t^3, R_\mu]\}\{R^\mu, R^\nu\})] + \frac{h_1}{2}\mathrm{Tr}(\Phi^\dagger\Phi)\mathrm{Tr}[(L^\mu)^2 + (R^\mu)^2] + h_2\,\mathrm{Tr}[|\Phi R^\mu|^2 + |L^\mu\Phi|^2] + 2h_3\,\mathrm{Tr}(\Phi R_\mu\Phi^\dagger L^\mu) \\
&+ g_4\{\mathrm{Tr}[L^\mu L^\nu L_\mu L_\nu] + \mathrm{Tr}[R^\mu R^\nu R_\mu R_\nu]\} + g_5\{\mathrm{Tr}[L^\mu L_\mu L^\nu L_\nu] + \mathrm{Tr}[R^\mu R_\mu R^\nu R_\nu]\} + g_6\,\mathrm{Tr}[R^\mu R_\mu]\mathrm{Tr}[L^\nu L_\nu] \\
&+ g_7\{\mathrm{Tr}[L^\mu L_\mu]\mathrm{Tr}[L^\nu L_\nu] + \mathrm{Tr}[R^\mu R_\mu]\mathrm{Tr}[R^\nu R_\nu]\}. \qquad (1)
\end{aligned}$$

Note that the locally chirally invariant linear sigma model emerges from the globally invariant Lagrangian (1) by setting $h_1 = h_2 = h_3 = g_3 = 0$, $g_2 = g_4 = g_5 = g_6 = g_7 \equiv g$.

In Eq. (1),

$$\Phi = (\sigma + i\eta_N)t^0 + (\vec{a}_0 + i\vec{\pi}) \cdot \vec{t} \tag{2}$$

contains scalar and pseudoscalar mesons, where t^0, $\vec{t}$ are the generators of $U(2)$ in the fundamental representation and η_N denotes the nonstrange content of the η meson. Vector and axial-vector mesons are contained in the left-handed and right-handed vector fields:

$$L^\mu = (\omega^\mu + f_1^\mu)t^0 + (\vec{\rho}^\mu + \vec{a}_1^\mu) \cdot \vec{t}, \tag{3a}$$

$$R^\mu = (\omega^\mu - f_1^\mu)t^0 + (\vec{\rho}^\mu - \vec{a}_1^\mu) \cdot \vec{t}, \tag{3b}$$

respectively. The covariant derivative

$$D^\mu\Phi = \partial^\mu\Phi - ig_1(L^\mu\Phi - \Phi R^\mu) - ieA^\mu[t^3, \Phi] \tag{4}$$

couples scalar and pseudoscalar degrees of freedom to vector and axial-vector ones as well as to the electromagnetic field A^μ. Note that local chiral invariance requires $g_1 \equiv g$. The left-handed and right-handed field strength tensors,

$$L^{\mu\nu} = \partial^\mu L^\nu - ieA^\mu[t^3, L^\nu] - \{\partial^\nu L^\mu - ieA^\nu[t^3, L^\mu]\}, \tag{5a}$$

$$R^{\mu\nu} = \partial^\mu R^\nu - ieA^\mu[t^3, R^\nu] - \{\partial^\nu R^\mu - ieA^\nu[t^3, R^\mu]\}, \tag{5b}$$

respectively, couple vector and axial-vector mesons to the electromagnetic field A^μ. Explicit breaking of the global symmetry is described by the term $\mathrm{Tr}[H(\Phi + \Phi^\dagger)] \equiv h_0\sigma$ ($h_0 = \text{const}$). The chiral anomaly is described by the term $c\,(\det\Phi + \det\Phi^\dagger)$ [3]. The model has been extended to include the nucleon field and its putative chiral partner; for details, see Refs. [13,20].

In the pseudoscalar and (axial-)vector sectors the identification of mesons with particles listed in Ref. [21] is straightforward, as already indicated in Eqs. (2), (3a), and (3b): the fields $\vec{\pi}$ and η_N correspond to the pion and the $SU(2)$ counterpart of the η meson, $\eta_N \equiv (\bar{u}u + \bar{d}d)/\sqrt{2}$, with a mass of about 700 MeV. This value can be obtained by "unmixing" the physical η and η' mesons, which also contain $\bar{s}s$ contributions. The fields ω^μ and $\vec{\rho}^\mu$ represent the $\omega(782)$ and $\rho(770)$ vector mesons, respectively, while the fields f_1^μ and $\vec{a}_1^\mu$ represent the $f_1(1285)$ and $a_1(1260)$ axial-vector mesons, respectively. (In principle, the physical ω and f_1 states also contain $\bar{s}s$ contributions, however their admixture is negligibly small.) Unfortunately, the identification of the σ and $\vec{a}_0$ fields is controversial, the possibilities being the pairs $\{f_0(600), a_0(980)\}$ and $\{f_0(1370), a_0(1450)\}$. As mentioned in the Introduction, we will refer to these two assignments as Scenarios I and II, respectively. We discuss the implications of these two scenarios in the following.

The inclusion of (axial-)vector mesons in effective models of QCD has been done also in other ways than the one presented here. Vector and axial-vector mesons have been included in chiral perturbation theory in Ref. [22]. While the mathematical expressions for the interaction terms turn out to be similar to our results, in our linear approach the number of parameters is smaller. In Ref. [23], the so-called hidden gauge formalism is used to introduce vector mesons, and subsequently axial-vector mesons, into a chiral Lagrangian with a nonlinear realization of chiral symmetry. In this case, the number of parameters is smaller. This approach is closely related to the locally chirally invariant models [6,7] (also called massive Yang-Mills approaches), which have been discussed in the Introduction as a motivation for the present work. We refer also to Ref. [24], where a comparative analysis of effective chiral Lagrangians for spin-1 mesons is presented.

One may raise the question whether vector-meson dominance (VMD) is still respected in the globally invariant linear sigma model (1). As outlined in Ref. [25], there are two ways to realize VMD in a linear sigma model. The standard version of VMD was introduced by Sakurai [26] and considers vector mesons as Yang-Mills gauge fields [27]. The gauge symmetry is explicitly broken by the vector-meson masses. Another realization of VMD was first explored by Lurie [28] whose theory contained a Lagrangian which was globally invariant. It is interesting to note that Lurie's Lagrangian contained direct couplings of the photon to pions and ρ mesons, as well as a $.\rho\text{-}\pi$ coupling. It was shown in Ref. [25] that the two representations of VMD are equivalent if the $\rho\text{-}\pi$ coupling $g_{\rho\pi\pi}$ equals the photon-ρ coupling g_ρ (the so-called "universal limit"). It was also shown that, if the underlying theory is globally invariant, the pion form factor at threshold $F_\pi(q^2 = 0) = 1$ for *any* value of the above mentioned couplings. On the other hand, in Sakurai's theory $F_\pi(q^2 = 0) \neq 1$ unless one demands $g_{\rho\pi\pi} =^! g_\rho$, or other parameters are adjusted in such a way that $F_\pi(q^2 = 0) = 1$. In other words, for *any* globally invariant model, and thus also for ours, one has the liberty of choosing different values for the photon-ρ and $\rho\text{-}\pi$ couplings, without violating VMD.

B. Tree-level masses

The Lagrangian (1) contains 16 parameters. However, the parameters g_k with $k = 3, \ldots, 7$ are not relevant for the results presented here so that the number of undetermined parameters decreases to 11:

$$m_0, \lambda_1, \lambda_2, m_1, g_1, g_2, c, h_0, h_1, h_2, h_3. \tag{6}$$

The squared tree-level masses of the mesons in our model contain a contribution arising from spontaneous symmetry breaking, proportional to ϕ^2. The value ϕ is the vacuum expectation value of the σ field and coincides with the

minimum of the potential that follows from Eq. (1). The σ field is the only field with the quantum numbers of the vacuum, $J^{PC} = 0^{++}$, i.e., the condensation of which does not lead to the breaking of parity, charge conjugation, and Lorentz invariance. The potential for the σ field reads explicitly

$$V(\sigma) = \frac{1}{2}(m_0^2 - c)\sigma^2 + \frac{1}{4}\left(\lambda_1 + \frac{\lambda_2}{2}\right)\sigma^4 - h_0\sigma, \quad (7)$$

and its minimum is determined by

$$0 = \left(\frac{dV}{d\sigma}\right)_{\sigma=\phi} = \left[m_0^2 - c + \left(\lambda_1 + \frac{\lambda_2}{2}\right)\phi^2\right]\phi - h_0. \quad (8)$$

Spontaneous symmetry breaking corresponds to the case when the potential $V(\phi)$ assumes its minimum for a nonvanishing value $\sigma = \phi \neq 0$. In order to determine the fluctuation of the σ field around the new vacuum, one shifts it by its vacuum expectation value $\phi \neq 0$, $\sigma \rightarrow \sigma + \phi$. The shift leads also to η_N-f_1 and $\vec{\pi}$-$\vec{a}_1$ mixing terms and thus to nondiagonal elements in the scattering matrix. These terms are removed from the Lagrangian by shifting the f_1 and $\vec{a}_1$ fields as follows:

$$\begin{aligned} f_1^\mu &\rightarrow f_1^\mu + Zw\partial^\mu\eta_N, \qquad \vec{a}_1^\mu \rightarrow \vec{a}_1^\mu + Zw\partial^\mu\vec{\pi}, \\ \eta_N &\rightarrow Z\eta_N, \qquad \vec{\pi} \rightarrow Z\vec{\pi}, \end{aligned} \quad (9)$$

where we defined the quantities

$$w := \frac{g_1\phi}{m_{a_1}^2}, \qquad Z := \left(1 - \frac{g_1^2\phi^2}{m_{a_1}^2}\right)^{-1/2}. \quad (10)$$

Note that the field renormalization of η_N and $\vec{\pi}$ guarantees the canonical normalization of the kinetic terms. This is necessary in order to interpret the Fourier components of the properly normalized one-meson states as creation or annihilation operators [6]. Note also that the ρ and ω masses as well as the f_1 and a_1 masses are degenerate in the globally as well as in the locally invariant model. Once the shift $\sigma \rightarrow \sigma + \phi$ and the transformations (9) have been performed, the mass terms of the mesons in the Lagrangian (1) read

$$m_\sigma^2 = m_0^2 - c + 3\left(\lambda_1 + \frac{\lambda_2}{2}\right)\phi^2, \quad (11)$$

$$m_{\eta_N}^2 = Z^2\left[m_0^2 + c + \left(\lambda_1 + \frac{\lambda_2}{2}\right)\phi^2\right] = m_\pi^2 + 2cZ^2, \quad (12)$$

$$m_{a_0}^2 = m_0^2 + c + \left(\lambda_1 + 3\frac{\lambda_2}{2}\right)\phi^2, \quad (13)$$

$$m_\pi^2 = Z^2\left[m_0^2 - c + \left(\lambda_1 + \frac{\lambda_2}{2}\right)\phi^2\right] \overset{(8)}{=} \frac{Z^2 h_0}{\phi}, \quad (14)$$

$$m_\omega^2 = m_\rho^2 = m_1^2 + \frac{\phi^2}{2}(h_1 + h_2 + h_3), \quad (15)$$

$$m_{f_1}^2 = m_{a_1}^2 = m_1^2 + g_1^2\phi^2 + \frac{\phi^2}{2}(h_1 + h_2 - h_3). \quad (16)$$

In the Appendix, we show the Lagrangian in the form when all shifts have been explicitly performed. From Eqs. (15) and (16), we obtain

$$m_{a_1}^2 = m_\rho^2 + g_1^2\phi^2 - h_3\phi^2. \quad (17)$$

The pion decay constant, f_π is determined from the axial current,

$$J_{A_\mu}^a = \frac{\phi}{Z}\partial_\mu\pi^a + \ldots \equiv f_\pi\partial_\mu\pi^a + \ldots \rightarrow \phi = Zf_\pi. \quad (18)$$

The large-N_c dependence of the parameters is given by

$$\begin{aligned} &g_1, g_2 \propto N_c^{-1/2}, \qquad \lambda_2, h_2, h_3, c \propto N_c^{-1}, \\ &\lambda_1, h_1 \propto N_c^{-2}, \qquad m_0^2, m_1^2 \propto N_c^0, \qquad h_0 \propto N_c^{1/2}. \end{aligned} \quad (19)$$

We remind the reader that a vertex of n quark-antiquark mesons scales as $N_c^{-(n-2)/2}$. As a consequence, the parameters g_1, g_2 scale as $N_c^{-1/2}$, because they are associated with a three-point vertex of quark-antiquark vector fields (of the kind ρ^3). Similarly, the parameters λ_2, h_2, h_3 scale as N_c^{-1}, because they are associated with quartic terms such as π^4 and $\pi^2\rho^2$. The parameter c is suppressed by a factor N_c although it enters quadratic masslike terms. This is due to the fact that the axial anomaly is suppressed in the large-N_c limit. As is evident from Eq. (12), the η_N meson would also be a Goldstone boson for $N_c \rightarrow \infty$. The parameters λ_1, h_1 also describe quartic interactions, but are further suppressed by a factor $1/N_c$ because of the trace structure of the corresponding terms in the Lagrangian. The quantities m_0^2, m_1^2 are mass terms and therefore scale as N_c^0. Then the pion decay constant f_π scales as $N_c^{1/2}$. The quantity h_0 scales as $N_c^{1/2}$ in order that m_π scales as N_c^0 as expected. Note that without any assumptions about the σ, a_0, and f_1, a_1 fields, we immediately obtain that their masses scale as N_c^0 and their decay widths as N_c^{-1}, as we shall see in the following section. Therefore, they must also correspond to quark-antiquark degrees of freedom.

There are, however, also approaches to the phenomenology of low-lying axial-vector mesons, such as the one in Ref. [29], where the Bethe-Salpeter equation is used to unitarize the scattering of vector and pseudoscalar mesons. Here, the Bethe-Salpeter kernel is given by the lowest-order effective Lagrangian. This leads to the dynamical generation of resonances, one of which has a pole mass of 1011 MeV and is consequently assigned to the $a_1(1260)$ meson. This unitarized approach is used in Ref. [30] to study the large-N_c behavior of the dynamically generated resonances, with the conclusion that the $a_1(1260)$ resonance is not a genuine quark-antiquark state.

However, it was shown in Ref. [14] that, while unitarizing the chiral Lagrangian by means of a Bethe-Salpeter study allows one to find poles in the complex plane and

identify them with physical resonances, it does not necessarily allow one to make a conclusion about the structure of those resonances in the large-N_c limit. In order to be able to draw correct conclusions, a Bethe-Salpeter study requires at least one additional term of higher-order not included in the Lagrangian of Refs. [29,30]. Alternatively, the Inverse amplitude method of Ref. [31] can be used.

A very similar approach to the one in Refs. [29,30] was also used in Ref. [32] where a very good fit to the τ decay data from the ALEPH Collaboration [33] was obtained by fine-tuning the subtraction point of a loop diagram. Note, however, that detuning the subtraction point by 5% will spoil the agreement with experimental data. Alternately, these data may be described by approaches with the $a_1(1260)$ meson as an explicit degree of freedom, such as the one in Ref. [12], where $a_1(1260)$ is a quark-antiquark state and where the experimental $a_1(1260)$ spectral function is fitted very well. In Ref. [12], $m_{a_1(1260)} \simeq 1150$ MeV and a full width $\Gamma_{a_1(1260)} \simeq 410$ MeV are obtained. Note that our results, as will be shown later, give very good results on the $a_1(1260)$ phenomenology, for example, in the $a_1(1260) \to \pi\gamma$ and $a_1(1260) \to \rho\pi$ decay channels, see Sec. IV A 3.

For the following discussion, it is interesting to note that the ρ meson mass can be split into two contributions:

$$m_\rho^2 = m_1^2 + \frac{\phi^2}{2}(h_1 + h_2 + h_3). \tag{20}$$

Without further assumptions, it is not possible to relate the quantity m_1^2 to microscopic condensates of QCD. However, invoking dilatation invariance, the term $\frac{m_1^2}{2}\,\mathrm{Tr}[(L^\mu)^2 + (R^\mu)^2]$ in Eq. (1) arises from a term $a\frac{G^2}{2}\,\mathrm{Tr}[(L^\mu)^2 + (R^\mu)^2]$ where G is the dilatation field and a a dimensionless constant. Upon shifting the dilatation field by $G \to G_0 + G$, with G_0 being the gluon condensate, one obtains the term in our Lagrangian upon identifying $m_1^2 = aG_0^2$. Thus, the quantity m_ρ^2 in Eq. (20) is expressed as a sum of a term which is directly proportional to the gluon condensate G_0, and a term which is directly proportional to the chiral condensate ϕ^2.

We shall require that none of the two contributions be negative: in fact, a negative $m_1^2 = aG_0^2$ would imply that the system is unstable when $\phi \to 0$; a negative $\frac{\phi^2}{2}(h_1 + h_2 + h_3)$ would imply that spontaneous chiral symmetry breaking decreases the ρ mass. This is clearly unnatural because the breaking of chiral symmetry generates a sizable effective mass for the light quarks, which is expected to positively contribute to the meson masses. This positive contribution is a feature of all known models (such as the Nambu–Jona-Lasinio model and constituent quark approaches). Indeed, in an important class of hadronic models (see Ref. [34] and references therein) the only and obviously positive contribution to the ρ mass is proportional to ϕ^2 (i.e., $m_1 = 0$).

In the vacuum, the very occurrence of chiral symmetry breaking can be also traced back to the interaction with the dilaton field: in fact, the quantity $-m_0^2\,\mathrm{Tr}(\Phi^\dagger\Phi)$, where $m_0^2 < 0$, arises from a dilatation-invariant interaction term of the form $bG^2\,\mathrm{Tr}(\Phi^\dagger\Phi)$ upon the identification $m_0^2 = bG_0^2$. This property also implies that the chiral condensate ϕ is proportional to the gluon condensate G_0, $\phi \sim G_0$. This means that the vacuum expression in Eq. (20) can be rewritten in the form $m_\rho^2 \sim \phi^2$, which resembles the Kawarabayashi-Suzuki-Fayyazuddin-Riazuddin relation [35]. However, the quantities G_0 are ϕ may vary independently from each other at nonzero temperature and density, thus generating a nontrivial behavior of m_ρ^2.

C. Equivalent set of parameters

Instead of the 11 parameters in Eq. (6), it is technically simpler to use the following, equivalent set of 11 parameters in the expressions for the physical quantities:

$$m_\pi, m_\sigma, m_{a_0}, m_{\eta_N}, m_\rho, m_{a_1}, Z, \phi, g_2, h_1, h_2. \tag{21}$$

The quantities m_π, m_ρ, m_{a_1} are taken as the mean values for the masses of the π, ρ, and a_1 meson, respectively, as given by the PDG [21]: $m_\pi = 139.57$ MeV, $m_\rho = 775.49$ MeV, and $m_{a_1} = 1230$ MeV. While m_π and m_ρ are measured to very good precision, this is not the case for m_{a_1}. The mass value given above is referred to as an "educated guess" by the PDG [21]. Therefore, we shall also consider a smaller value, as suggested, e.g., by the results of Ref. [12]. We shall see that, although the overall picture remains qualitatively unchanged, the description of the decay width of a_1 into $\rho\pi$ can be substantially improved.

As outlined in Ref. [11], the mass of the η_N meson can be calculated using the mixing of strange and nonstrange contributions in the physical fields η and $\eta'(958)$:

$$\begin{aligned} \eta &= \eta_N \cos\varphi + \eta_S \sin\varphi, \\ \eta' &= -\eta_N \sin\varphi + \eta_S \cos\varphi, \end{aligned} \tag{22}$$

where η_S denotes a pure $\bar{s}s$ state and $\varphi \simeq -36°$ [36]. In this way, we obtain the value $m_{\eta_N} = 716$ MeV. Given the well-known uncertainty of the value of φ, one could also consider other values, e.g., $\varphi = -41.4°$, as published by the KLOE Collaboration [37]. In this case, $m_{\eta_N} = 755$ MeV. The variation of the η_N mass does not change the results significantly.

The quantities ϕ and Z are linked to the pion decay constant as $\phi/Z = f_\pi = 92.4$ MeV. Therefore, the following six quantities remain as free parameters:

$$m_\sigma, m_{a_0}, Z, g_2, h_1, h_2. \tag{23}$$

The masses m_σ and m_{a_0} depend on the scenario adopted for the scalar mesons.

At the end of this subsection we report three useful formulas which link the parameters g_1, h_3, and m_1 of the original set (6) to the second set of parameters (21) [see also Eq. (10)]:

$$g_1 = g_1(Z) = \frac{m_{a_1}}{Z f_\pi}\sqrt{1-\frac{1}{Z^2}}, \tag{24}$$

$$h_3 = h_3(Z) = \frac{m_{a_1}^2}{Z^2 f_\pi^2}\left(\frac{m_\rho^2}{m_{a_1}^2}-\frac{1}{Z^2}\right), \tag{25}$$

$$\begin{aligned} m_1^2 &= m_1^2(Z, h_1, h_2) \\ &= \tfrac{1}{2}[m_\rho^2 + m_{a_1}^2 - Z^2 f_\pi^2 (g_1^2 + h_1 + h_2)]. \end{aligned} \tag{26}$$

III. DECAY WIDTHS AND $\pi\pi$ SCATTERING LENGTHS

In this section, we quote the formulas for the decay widths and the $\pi\pi$ scattering lengths and specify their dependence on the parameters m_σ, m_{a_0}, Z, g_2, h_1, and h_2. Using the scaling behavior (19) we obtain that all strong decays and scattering lengths scale as N_c^{-1}, as expected.

For future use we introduce the momentum function

$$\begin{aligned} k(m_a, m_b, m_c) = &\frac{1}{2m_a} \\ &\times \sqrt{m_a^4 - 2m_a^2(m_b^2+m_c^2) + (m_b^2 - m_c^2)^2} \\ &\times \theta(m_a - m_b - m_c). \end{aligned} \tag{27}$$

In the decay process $a \to b + c$, with masses m_a, m_b, m_c, respectively, the quantity $k(m_a, m_b, m_c)$ represents the modulus of the three-momentum of the outgoing particles b and c in the rest frame of the decaying particle a. The theta function ensures that the decay width vanishes below threshold.

A. The $\rho \to \pi\pi$ decay width

The decay width for $\rho \to \pi\pi$ reads

$$\begin{aligned} \Gamma_{\rho\to\pi\pi}(Z, g_2) = &\frac{m_\rho^5}{48\pi m_{a_1}^4} \\ &\times \left[1 - \left(\frac{2m_\pi}{m_\rho}\right)^2\right]^{3/2}\left[g_1 Z^2 + (1-Z^2)\frac{g_2}{2}\right]^2. \end{aligned} \tag{28}$$

The experimental value is $\Gamma_{\rho\to\pi\pi}^{(\mathrm{exp})} = (149.1 \pm 0.8)$ MeV [21]. The small experimental error can be neglected and the central value is used as a further constraint allowing us to fix the parameter g_2 as function of Z:

$$g_2 = g_2(Z) = \frac{2}{Z^2-1}\left(g_1 Z^2 \pm \frac{4m_{a_1}^2}{m_\rho}\sqrt{\frac{3\pi\Gamma_{\rho\to\pi\pi}^{(\mathrm{exp})}}{(m_\rho^2 - 4m_\pi^2)^{3/2}}}\right). \tag{29}$$

Note that all input values in Eq. (29) are experimentally known [21]. The parameter $g_1 = g_1(Z)$ is fixed via Eq. (24).

As apparent from Eq. (29), two solutions for g_2 are obtained. The solution with the positive sign in front of the square root may be neglected because it leads to unphysically large values for the $a_1 \to \rho\pi$ decay width, which is another quantity predicted by our study that also depends on g_2 [see Eq. (40)]. For example, the value $Z = 1.6$ (see below) would lead to $g_2 \cong 40$ which in turn would give $\Gamma_{a_1\to\rho\pi} \cong 14$ GeV—clearly an unphysically large value. Therefore, we will take the solution for g_2 with the negative sign in front of the square root. In this case, reasonable values for both g_2 (see Sec. IV A 1) and $\Gamma_{a_1\to\rho\pi}$ (see Sec. IV A 3) are obtained.

B. The $f_1 \to a_0\pi$ decay width

The decay width $f_1 \to a_0\pi$ reads

$$\begin{aligned} \Gamma_{f_1\to a_0\pi}(m_{a_0}, Z, h_2) = &\frac{g_1^2 Z^2}{2\pi}\frac{k^3(m_{f_1}, m_{a_0}, m_\pi)}{m_{f_1}^2 m_{a_1}^4} \\ &\times \left[m_\rho^2 - \frac{1}{2}(h_2+h_3)\phi^2\right]^2. \end{aligned} \tag{30}$$

There is a subtle point to comment on here. When the quark-antiquark a_0 state of our model is identified as the $a_0(980)$ meson of the PDG compilation (Scenario I), then this decay width can be used to fix the parameter h_2 as function of Z, $h_2 \equiv h_2(Z)$, by using the corresponding experimental value $\Gamma_{f_1\to a_0\pi}^{(\mathrm{exp})} = (8.748 \pm 2.097)$ MeV [21].

$$\begin{aligned} h_2 &= h_2(Z) \\ &= \frac{2}{\phi^2}\left(m_\rho^2 - \frac{h_3}{2}\phi^2 \pm \frac{m_{f_1} m_{a_0}^2}{g_1 Z}\sqrt{\frac{2\pi\Gamma_{f_1\to a_0\pi}^{(\mathrm{exp})}}{k^3(m_{f_1}, m_{a_0}, m_\pi)}}\right). \end{aligned} \tag{31}$$

Again, there are two solutions, just as in the case of the parameter g_2. How strongly the somewhat uncertain experimental value of $\Gamma_{f_1\to a_0\pi}$ influences the possible values of h_2, depends on the choice of the sign in front of the square root in Eq. (31). Varying $\Gamma_{f_1\to a_0\pi}$ within its experimental range of uncertainty changes the value of h_2 by an average of 25% if the negative sign is chosen, but the same variation of $\Gamma_{f_1\to a_0\pi}$ changes h_2 by an average of only 6% if the positive sign is considered. This is due to the fact that the solution with the positive square root sign yields larger values of $h_2 \sim 80$, while the solution with the negative sign leads to $h_2 \sim 20$. The absolute change of h_2 is the same in both cases. Our calculations have shown that using the

negative sign in front of the square root yields a too small value of the η-η' mixing angle $\varphi \cong -9°$. This follows by inserting h_2 into Eq. (33) so that it is removed as a degree of freedom (i.e., replaced by Z) and calculating the mixing angle φ from Eq. (32) using the experimental value of the $a_0 \to \eta\pi$ decay amplitude from Ref. [38]. For this reason, we only use the positive sign in front of the square root in Eq. (31), i.e., the constraint leading to higher values of h_2. Then $\varphi \cong -41.8°$ is obtained, in very good agreement with the central value quoted by the KLOE Collaboration [37], $\varphi \cong -41.4°$ (see also Sec. IV A 1).

It may be interesting to note that only the (disregarded) lower value of h_2 leads to the expected behavior of the parameter h_1 which [according to Eq. (19)] should be large-N_c suppressed: the lower value of h_2 yields $h_1 = 1.8$ whereas the higher value of h_2 yields $h_1 = -68$ (see Sec. IV A 1).

Note that if the quark-antiquark a_0 meson of our model is identified as the $a_0(1450)$ meson of the PDG compilation (Scenario II) then the described procedure of replacing h_2 by Z using Eq. (31) is no longer applicable because the decay $f_1 \to a_0\pi$ is kinematically not allowed and its counterpart $a_0 \to f_1\pi$ has not been measured.

C. The $a_0 \to \eta\pi$ and $a_0 \to \eta'\pi$ decay amplitudes

Our $N_f = 2$ Lagrangian contains the unphysical field η_N. However, by making use of Eq. (22) and invoking the Okubo-Zweig-Iizuka rule, it is possible to calculate the decay amplitude for the physical process $a_0 \to \eta\pi$ as

$$A_{a_0\eta\pi} = \cos\varphi A_{a_0\eta_N\pi}. \tag{32}$$

From Eq. (1) the formula for the decay amplitude containing the nonstrange η_N field is

$$A_{a_0\eta_N\pi}(m_{a_0}, Z, h_2) = \frac{1}{Zf_\pi}\left\{m_{\eta_N}^2 - m_{a_0}^2 + \left(1 - \frac{1}{Z^2}\right) \times \left[1 - \frac{1}{2}\frac{Z^2\phi^2}{m_{a_1}^2}(h_2 - h_3)\right] \times (m_{a_0}^2 - m_\pi^2 - m_\eta^2)\right\}. \tag{33}$$

Note that Eq. (33) contains the unmixed mass m_{η_N} which enters when expressing the coupling constants in terms of the parameters (21), as well as the physical mass $m_\eta = 547.8$ MeV. The latter arises because the derivative couplings in the Lagrangian lead to the appearance of scalar invariants formed from the four-momenta of the particles emerging from the decay, which can be expressed in terms of the physical (invariant) masses.

The decay width $\Gamma_{a_0\to\eta\pi}$ follows from Eq. (32) by including a phase space factor:

$$\Gamma_{a_0\to\eta\pi}(m_{a_0}, Z, h_2) = \frac{k(m_{a_0}, m_\eta, m_\pi)}{8\pi m_{a_0}^2} \times [A_{a_0\eta\pi}(m_{a_0}, Z, h_2)]^2. \tag{34}$$

In the case of Scenario I, in which $a_0 \equiv a_0(980)$, we shall compare the decay amplitude $A_{a_0\eta\pi}$, Eq. (32), with the corresponding experimental value deduced from Crystal Barrel data: $A_{a_0\eta\pi}^{(\mathrm{exp})} = (3330 \pm 150)$ MeV [38]. This is preferable to the use of the decay width quoted by the PDG [21] for $a_0(980)$, which refers to the mean peak width, an unreliable quantity due to the closeness of the kaon-kaon threshold.

In the case of Scenario II, in which $a_0 \equiv a_0(1450)$, it is also possible to calculate the decay width $a_0(1450) \to \eta'\pi$, using the Okubo-Zweig-Iizuka rule. The amplitude $A_{a_0\eta'\pi}(m_{a_0}, Z, h_2)$ is obtained following the same steps as in the previous case, Eq. (33):

$$A_{a_0\eta'\pi}(m_{a_0}, Z, h_2) = -\frac{\sin\varphi}{Zf_\pi}\left\{m_{\eta_N}^2 - m_{a_0}^2 + \left(1 - \frac{1}{Z^2}\right) \times \left[1 - \frac{1}{2}\frac{Z^2\phi^2}{m_{a_1}^2}(h_2 - h_3)\right] \times (m_{a_0}^2 - m_\pi^2 - m_{\eta'}^2)\right\}, \tag{35}$$

where the difference compared to Eqs. (32) and (33) is the prefactor $-\sin\varphi$ and the physical η' mass $m_{\eta'} = 958$ MeV. The corresponding decay width reads

$$\Gamma_{a_0(1450)\to\eta'\pi}(m_{a_0}, Z, h_2) = \frac{k(m_{a_0}, m_{\eta'}, m_\pi)}{8\pi m_{a_0}^2} \times [A_{a_0\eta'\pi}(m_{a_0}, Z, h_2)]^2. \tag{36}$$

D. The $a_1 \to \pi\gamma$ decay width

We obtain the following formula for the $a_1 \to \pi\gamma$ decay width:

$$\Gamma_{a_1\to\pi\gamma}(Z) = \frac{e^2}{96\pi}(Z^2 - 1)m_{a_1}\left[1 - \left(\frac{m_\pi}{m_{a_1}}\right)^2\right]^3. \tag{37}$$

Note that the $a_1 \to \pi\gamma$ decay width depends only on the renormalization constant Z. In fact, it is generated via the a_1-π mixing and vanishes in the limit $Z \to 1$. (A similar mechanism for this decay is described in Ref. [22].) The fact that we include photons following the second realization of VMD described in Ref. [25] renders this process possible in our model. Using $\Gamma_{a_1\to\pi\gamma}^{(\mathrm{exp})} = (0.640 \pm 0.246)$ MeV [21], one obtains $Z = 1.67 \pm 0.2$. Unfortunately, the experimental error for the quantity $\Gamma_{a_1\to\pi\gamma}$ is large. Given that almost all quantities of interest depend very strongly on Z, a better experimental knowledge of this

decay would be useful to constrain Z. In the study of Scenario I this decay width will be part of a χ^2 analysis, but still represents the main constraint for Z.

E. The $\sigma \to \pi\pi$ decay width

We obtain the following formula:

$$\Gamma_{\sigma\to\pi\pi}(m_\sigma, Z, h_1, h_2) = \frac{3}{32\pi m_\sigma}\sqrt{1-\left(\frac{2m_\pi}{m_\sigma}\right)^2} \times \left\{\frac{m_\sigma^2 - m_\pi^2}{Zf_\pi} - \frac{g_1^2 Z^3 f_\pi}{m_{a_1}^4}\left[m_\rho^2 - \frac{\phi^2}{2}(h_1+h_2+h_3)\right] \times (m_\sigma^2 - 2m_\pi^2)\right\}^2. \quad (38)$$

It is apparent from Eqs. (19) that the sigma decay width decreases as the number of colors N_c increases. Thus, the sigma field in our model is a $\bar{q}q$ state [31]. In Scenario I we have assigned the σ field as $f_0(600)$, correspondingly we are working with the assumption that $f_0(600)$ [as well as $a_0(980)$] is a $\bar{q}q$ state. In Scenario II, the same assumption is valid for the $f_0(1370)$ and $a_0(1450)$ states.

Note that in Eq. (38) the first term in braces arises from the scalar $\sigma\pi\pi$ vertex, while the second term comes from the coupling of the σ to the a_1, which becomes a derivatively coupled pion after the shift (9). Because of the different signs, these two terms interfere destructively. As the decay width of a light σ meson into two pions can be very well reproduced in the linear sigma model without vector mesons (corresponding to the case $g_1 \to 0$), this interference prevents obtaining a reasonable value for this decay width in the present model with vector mesons, see Sec. IV A 2. This problem does not occur for a heavy σ meson, see Sec. IV B 3 and Ref. [39].

F. The $a_1 \to \sigma\pi$ decay width

The formula for the decay width reads

$$\Gamma_{a_1\to\sigma\pi}(m_\sigma, Z, h_1, h_2) = \frac{k^3(m_{a_1}, m_\sigma, m_\pi)}{6\pi m_{a_1}^6} g_1^2 Z^2\left[m_\rho^2 - \frac{\phi^2}{2}(h_1+h_2+h_3)\right]^2. \quad (39)$$

G. The $a_1 \to \rho\pi$ decay width

Let P be the four-momentum of the a_1 meson, K_1 the four-momentum of the ρ meson and K_2 the four-momentum of the pion. Then the following formula for the $a_1 \to \rho\pi$ decay width is obtained:

$$\Gamma_{a_1\to\rho\pi}(Z) = \frac{k(m_{a_1}, m_\rho, m_\pi)}{12\pi m_{a_1}^2}\left[(h_{\mu\nu})^2 - \frac{(h_{\mu\nu}K_1^\nu)^2}{m_\rho^2} - \frac{(h_{\mu\nu}P^\mu)^2}{m_{a_1}^2} + \frac{(h_{\mu\nu}P^\mu K_1^\nu)^2}{m_\rho^2 m_{a_1}^2}\right], \quad (40)$$

where $h_{\mu\nu}$ is the vertex following from the relevant part of the Lagrangian (1) that reads

$$h_{\mu\nu} = Z^2 f_\pi\left\{(g_1^2 - h_3)g_{\mu\nu} + \frac{g_1 g_2}{m_{a_1}^2} \times [K_{1\mu}K_{2\nu} + K_{2\mu}P_\nu - K_2\cdot(K_1+P)g_{\mu\nu}]\right\} \quad (41)$$

and

$$K_1\cdot K_2 = \frac{m_{a_1}^2 - m_\rho^2 - m_\pi^2}{2},$$
$$P\cdot K_2 = m_{a_1}E_\pi \equiv m_{a_1}\sqrt{k^2+m_\pi^2}.$$

Thus, we have

$$h_{\mu\nu}^2 = Z^4 f_\pi^2\left\{4(g_1^2-h_3)^2 + \frac{g_1^2 g_2^2}{m_{a_1}^4}[m_{a_1}^4 + m_\pi^4 + m_\rho^4 + m_\pi^2 m_\rho^2 + m_{a_1}^2(m_\pi^2 - 2m_\rho^2) + 3(m_{a_1}^2 - m_\rho^2 - m_\pi^2)m_{a_1}E_\pi] - 3\frac{g_1 g_2(g_1^2-h_3)}{m_{a_1}^2}(m_{a_1}^2 - m_\rho^2 - m_\pi^2 + 2m_{a_1}E_\pi)\right\},$$

$$(h_{\mu\nu}K_1^\nu)^2 = Z^4 f_\pi^2\left\{(g_1^2-h_3)^2 m_\rho^2 + \frac{g_1^2 g_2^2}{4m_{a_1}^4}[(m_\pi^2 - m_\rho^2)^2(m_\pi^2 + m_\rho^2 - 2m_{a_1}^2) + (m_\pi^2 + m_\rho^2)m_{a_1}^4 - 4(m_{a_1}^2 - m_\rho^2 - m_\pi^2)m_{a_1}^2 E_\rho E_\pi] + \frac{g_1 g_2(g_1^2-h_3)}{m_{a_1}^2}\left[(m_{a_1}^2 - m_\pi^2)m_{a_1}E_\rho - 2m_{a_1}m_\rho^2\left(E_\pi + \frac{E_\rho}{2}\right)\right]\right\},$$

$$(h_{\mu\nu}P^\mu)^2 = Z^4 f_\pi^2\left\{(g_1^2-h_3)^2 m_{a_1}^2 + \frac{g_1^2 g_2^2}{4m_{a_1}^4}[(m_{a_1}^2 - m_\pi^2)^2(m_{a_1}^2 + m_\pi^2 - 2m_\rho^2) + (m_\pi^2 + m_{a_1}^2)m_\rho^4 - 4(m_{a_1}^2 - m_\rho^2 - m_\pi^2)m_{a_1}^2 E_\rho E_\pi] + \frac{g_1 g_2(g_1^2-h_3)}{m_{a_1}^2}[2m_{a_1}^2 E_\rho E_\pi - (m_{a_1}^2 - m_\rho^2 - m_\pi^2)m_{a_1}^2]\right\},$$

$$(h_{\mu\nu}P^\mu K_1^\nu)^2 = (g_1^2 - h_3)^2 Z^4 f_\pi^2 m_{a_1}^2 E_\rho^2.$$

H. The tree-level scattering lengths

The partial wave decomposition [40] leads to the following formula for the s-wave $I = 0$ pion-pion scattering length a_0^0 (in units of m_π^{-1}):

$$a_0^0(Z, m_\sigma, h_1) = \frac{1}{4\pi}\Bigg(2g_1^2 Z^4 \frac{m_\pi^2}{m_{a_1}^4}\Big\{m_\rho^2 + \frac{\phi^2}{16}[12g_1^2 - 2(h_1+h_2) - 14h_3]\Big\} - \frac{5}{8}\frac{Z^2 m_\sigma^2 - m_\pi^2}{f_\pi^2} - \frac{3}{2}\Big\{g_1^2 Z^2 \phi \frac{m_\pi^2}{m_{a_1}^4}\Big[2m_{a_1}^2 + m_\rho^2 - \frac{\phi^2}{2}(h_1+h_2+h_3)\Big] - \frac{Z^2 m_\sigma^2 - m_\pi^2}{2\phi}\Big\}^2 \frac{1}{4m_\pi^2 - m_\sigma^2} + \Big\{g_1^2 Z^2 \phi \frac{m_\pi^2}{m_{a_1}^4}\Big[m_\rho^2 - \frac{\phi^2}{2}(h_1+h_2+h_3)\Big] + \frac{Z^2 m_\sigma^2 - m_\pi^2}{2\phi}\Big\}^2 \frac{1}{m_\sigma^2}\Bigg). \tag{42}$$

We use the value $a_0^{0(\mathrm{exp})} = 0.218 \pm 0.020$ in accordance with the 2003 and 2004 data from the NA48/2 Collaboration [41].

An analogous calculation leads to the s-wave $I = 2$ pion-pion scattering length a_0^2:

$$a_0^2(Z, m_\sigma, h_1) = -\frac{1}{4\pi}\Bigg(\frac{Z^2 m_\sigma^2 - m_\pi^2}{4f_\pi^2} + g_1^2 Z^4 \frac{m_\pi^2}{m_{a_1}^4}\Big[m_\rho^2 - \frac{\phi^2}{2}(h_1+h_2+h_3)\Big] - \Big\{g_1^2 Z^2 \phi \frac{m_\pi^2}{m_{a_1}^4}\Big[m_\rho^2 - \frac{\phi^2}{2}(h_1+h_2+h_3)\Big] + \frac{Z^2 m_\sigma^2 - m_\pi^2}{2\phi}\Big\}^2 \frac{1}{m_\sigma^2}\Bigg). \tag{43}$$

The experimental result for a_0^2 from the NA48/2 Collaboration is $a_0^{2(\mathrm{exp})} = -0.0457 \pm 0.0125$ [41]. Note that the $\pi\pi$ scattering lengths were also studied away from threshold in Ref. [42], in a model quite similar to ours.

IV. STUDY OF DIFFERENT SCENARIOS FOR THE STRUCTURE OF SCALAR MESONS

In this section we discuss two different interpretations of the scalar mesons. The following subsection describes the results obtained when $f_0(600)$ and $a_0(980)$ are interpreted as scalar quarkonia (Scenario I). Then we discuss the results obtained when $f_0(1370)$ and $a_0(1450)$ are interpreted as scalar quarkonia (Scenario II).

A. Scenario I: light scalar quarkonia

1. Fit procedure

As a first step we utilize the central value of the experimental result $\Gamma_{\rho\to\pi\pi}^{(\mathrm{exp})} = 149.1$ MeV [21] in order to express the parameter g_2 as a function of Z via Eq. (29). Moreover, we fix the mass $m_{a_0} = 0.98$ GeV [21] and we also use the central value $\Gamma_{f_1\to a_0\pi}(Z, h_2) = 8.748$ MeV to express h_2 as a function of Z. The results are practically unaffected by the 6% uncertainty in h_2 originating from the uncertainty in $\Gamma_{f_1\to a_0\pi}$, see Eq. (31).

As a result, the set of free parameters in Eq. (23) is further reduced to three parameters:

$$Z, m_\sigma, h_1. \tag{44}$$

Note that in this scenario the field σ is identified with the resonance $f_0(600)$, but the experimental uncertainty on its mass is so large that it does not allow us to fix m_σ. We therefore keep m_σ as a free parameter.

We now determine the parameters Z, h_1, and m_σ using known data on the $a_1 \to \pi\gamma$ decay width (37) and on the $\pi\pi$ scattering lengths a_0^0 and a_0^2 reported in Eqs. (42) and (43). This is a system of three equations with three variables and can be solved uniquely. We make use of the χ^2 method in order to determine not only the central values for our parameters but also their error intervals:

$$\chi^2(Z, m_\sigma, h_1) = \Bigg(\frac{\Gamma_{a_1\to\pi\gamma}(Z) - \Gamma_{a_1\to\pi\gamma}^{(\mathrm{exp})}}{\triangle\Gamma_{\mathrm{decay}}^{(\mathrm{exp})}}\Bigg)^2 + \sum_{i\in\{0,2\}}\Bigg(\frac{a_0^i(Z, m_\sigma, h_1) - a_0^{i(\mathrm{exp})}}{\triangle a_0^{i(\mathrm{exp})}}\Bigg)^2. \tag{45}$$

The errors for the model parameters are calculated as the square roots of the diagonal elements of the inverted Hessian matrix obtained from $\chi^2(Z, m_\sigma, h_1)$. The minimal value is obtained for $\chi^2 = 0$, as expected given that the parameters are determined from a uniquely solvable system of equations. The values of the parameters are as follows:

$$Z = 1.67 \pm 0.2, \qquad m_\sigma = (332 \pm 456)\ \mathrm{MeV}, \qquad h_1 = -68 \pm 338. \tag{46}$$

Clearly, the error intervals for m_σ and h_1 are very large. Fortunately, it is possible to constrain the h_1 error interval as follows. As described at the end of Sec. II B, the ρ mass squared contains two contributions—the bare mass term m_1^2 and the quark condensate contribution ($\sim \phi^2$). The contribution of the quark condensate is special for the

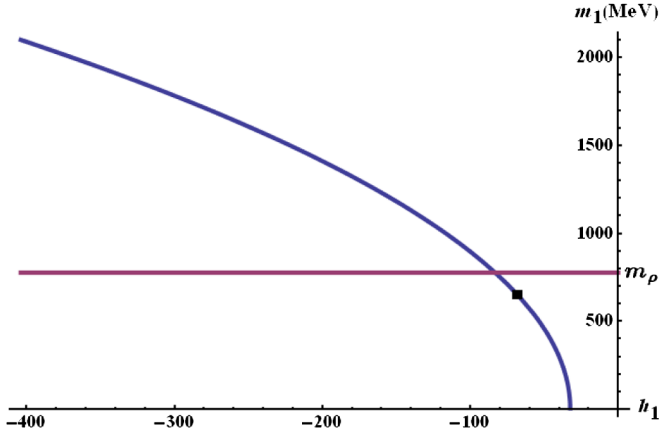

FIG. 1 (color online). m_1 as function of h_1, constrained at the central value of $Z = 1.67$. The black dot marks the position of central values $h_1 = -68$ and $m_1 = 652$ MeV.

globally invariant sigma model; in the locally invariant model m_ρ is always equal to m_1 [8]. Each of these contributions should have at most the value of 775.49 MeV ($= m_\rho$) because otherwise either the bare mass or the quark condensate contribution to the rho mass would be negative, which appears to be unphysical. A plot of the function $m_1 = m_1(Z, h_1, h_2(Z))$, see Eq. (26), for the central values of $Z = 1.67$ and $\Gamma^{(\mathrm{exp})}_{f_1 \to a_0 \pi} = 8.748$ MeV is shown in Fig. 1.

Note that varying the value of $\Gamma^{(\mathrm{exp})}_{f_1 \to a_0 \pi}$ within its experimental boundaries would only very slightly change h_1 by ± 4 and this parameter is thus unaffected by the experimental error for $\Gamma^{(\mathrm{exp})}_{f_1 \to a_0 \pi}$. If the value of m_1 was known exactly, then Eq. (26) would allow us to constrain h_1 via Z. However, given that at this point we can only state that $0 \leq m_1 \leq m_\rho$, for each Z one may consider all values of h_1 between two boundaries, one obtained from the condition $m_1(Z, h_1, h_2(Z)) \equiv 0$ and another obtained from the condition $m_1(Z, h_1, h_2(Z)) \equiv m_\rho$. For example, using the central value of $Z = 1.67$, we obtain $-83 \leq h_1 \leq -32$. The lower boundary follows from $m_1 \equiv m_\rho$ and the upper boundary from $m_1 \equiv 0$, see Fig. 1. Note that the central value $h_1 = -68$ from Eq. (46) corresponds to $m_1 = 652$ MeV. If the minimal value of $Z = 1.47$ is used, then $h_1 = -112$ is obtained from $m_1 \equiv m_\rho$ and $h_1 = -46$ from $m_1 \equiv 0$. Thus, $-112 \leq h_1 \leq -46$ for $Z = 1.47$. Analogously, $-64 \leq h_1 \leq -24$ is obtained for the maximal value $Z = 1.87$.

Clearly, each lower boundary for h_1 is equivalent to $m_1 \equiv m_\rho$ and each upper boundary for h_1 is equivalent to $m_1 \equiv 0$. Thus, in the following we will only state the values of Z and m_1; h_1 can always be calculated using Eq. (26). In this way, the dependence of our results on m_1 and thus on the origin of the ρ mass will be exhibited.

The value of m_σ can be constrained in a way similar to h_1 using the scattering length a_0^0; the scattering length a_0^2 possesses a rather large error interval making it unsuitable to constrain m_σ. Figure 2 shows the different values for a_0^0 and a_0^2 depending on the choice of Z and m_1.

It is obvious that the value of a_0^0 is only consistent with the NA48/2 value [41], if m_σ is in the interval [288, 477] MeV, i.e., $m_\sigma = 332^{+145}_{-44}$ MeV. This value for m_σ follows if the parameters Z and m_1 are varied within the allowed boundaries. If we only consider the a_0^0 curve that is obtained for the central values of Z and m_1, a much more constrained value of $m_\sigma = 332^{+24}_{-13}$ MeV follows from Fig. 2. We will be working with the broader interval of m_σ. Even then, constraining m_1 to the interval $[0, m_\rho]$, the error bars for m_σ are reduced by at least a factor of 3 in comparison to the result (46) following from the χ^2 calculation.

We summarize our results for the parameters Z and m_σ:

$$Z = 1.67 \pm 0.2, \qquad m_\sigma = 332^{+145}_{-44}\ \mathrm{MeV}.$$

The central values of all parameters of the original set (6)

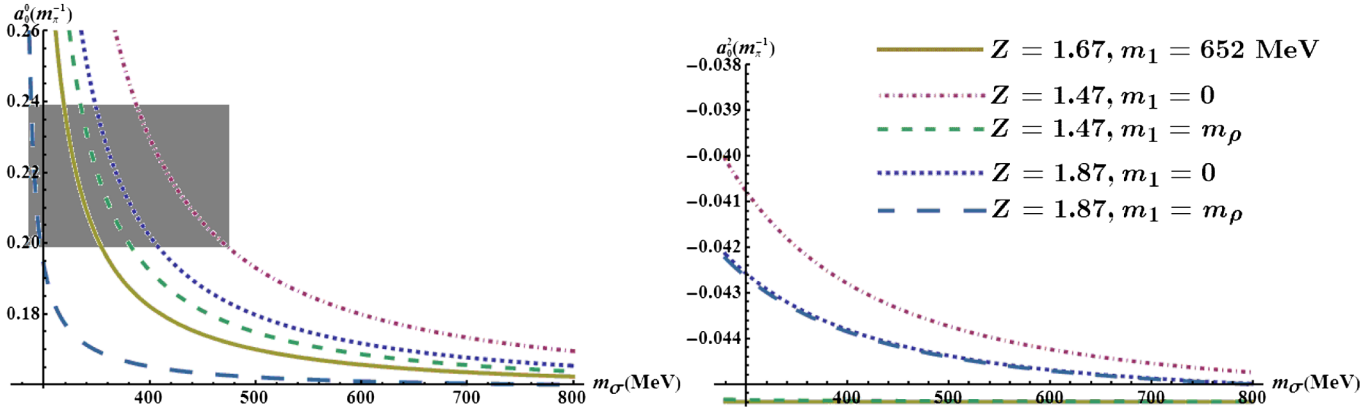

FIG. 2 (color online). Scattering lengths a_0^0 and a_0^2 as function of m_σ (the shaded band corresponds to the NA48/2 value of a_0^0; no error interval is shown for a_0^2 due to interval size [41]).

TABLE I. Central values of parameters for Scenario I.

Parameter	m_σ	h_1	h_2	h_3
Value	332 MeV	-68	80	2.4
Parameter	g_1	g_2	m_0	m_1
Value	6.4	3.1	210 MeV	652^{+123}_{-652} MeV
Parameter	λ_1	λ_2	c	h_0
Value	-14	33	88 744 MeV^2	1×10^6 MeV^3

are given in Table I. They follow from the χ^2 fit (m_σ, h_1), via decay width constraints (h_2, g_2), and from Eqs. (11)–(16), (24), and (25). The central values of Z, m_σ, and h_1, Eq. (46), have been used to calculate all other parameters. We neglect the errors, apart from those of m_1, which in this scenario vary in a large range.

Note that the values of a_0^2 depend strongly on the choice of the parameters Z and m_1. Whereas for the central values of Z and m_1 this scattering length is constant and has the value $a_0^2 = -0.0454$, its value increases if Z and m_1 are considered at their respective boundaries, see Fig. 2.

The value of Z alone allows us to calculate certain decay widths in the model. For example, as a consistency check we obtain $\Gamma_{a_1\to\pi\gamma} = 0.640^{+0.261}_{-0.231}$ MeV which is in good agreement with the experimental result. Also, given that the $a_0 \to \eta_N \pi$ decay amplitude only depends on Z, it is possible to calculate the value of this amplitude, Eq. (33). For $Z = 1.67$, we obtain $A_{a_0\to\eta\pi} = 3939$ MeV for the decay amplitude $a_0 \to \eta\pi$ involving the physical η field if the η-η' mixing angle of $\varphi = -36°$ [36] is taken. The Crystal Barrel data [38] read $A^{(\mathrm{exp})}_{a_0\to\eta\pi} = 3330$ MeV and hence there is an approximate discrepancy of 20%. If the KLOE Collaboration [37] value of $\varphi = -41.4°$ is considered, then the value of $A_{a_0\to\eta\pi} = 3373$ MeV follows—in perfect agreement with the Crystal Barrel value. From this we conclude that this scenario prefers a relatively large value of the η-η' mixing angle. In fact, if we use the Crystal Barrel value $A^{(\mathrm{exp})}_{a_0\to\eta\pi} = 3330$ MeV as input, we would predict $\varphi = -41.8°$ for the central value of Z as well as $\varphi = -42.3°$ and $\varphi = -41.6°$ for the highest and lowest values of Z, respectively, i.e., $\varphi = -41.8^{\circ\,+0.2^\circ}_{-0.5^\circ}$. This is in excellent agreement with the KLOE Collaboration result $\varphi = -41.4° \pm 0.5°$ but also with the results from approaches using the Bethe-Salpeter formalism, such as the one in Ref. [43].

2. The decay $\sigma \to \pi\pi$

The sigma decay width $\Gamma_{\sigma\to\pi\pi}$ depends on all three parameters Z, m_1 (originally h_1), and m_σ. In Fig. 3, we show the dependence of this decay width on the sigma mass for fixed values of Z and m_1, varying the latter within their respective boundaries.

Generally, the values that we obtain are too small when compared to the PDG data [21] and to other calculations of the sigma meson decay width, such as the one performed

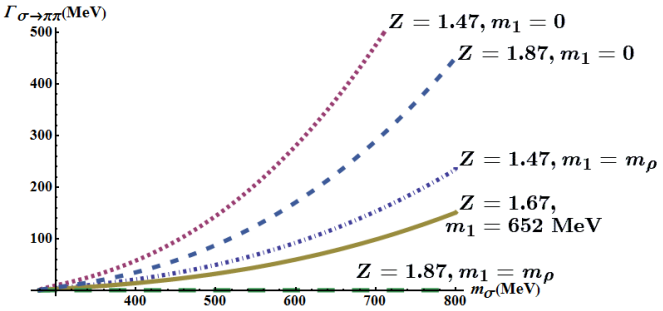

FIG. 3 (color online). $\Gamma_{\sigma\to\pi\pi}$ as function of m_σ for different values of Z and m_1. The PDG [21] notes $\Gamma_\sigma =$ (600–1000) MeV; the results from the chiral perturbation theory suggest $\Gamma_\sigma = 544$ MeV [44] and $\Gamma_\sigma = 510$ MeV [45].

by Leutwyler *et al.* [44] who found $\Gamma_{\sigma\to\pi\pi}/2 = 272^{+9}_{-12.5}$ MeV and Peláez *et al.* [45] who found $\Gamma_{\sigma\to\pi\pi}/2 = (255 \pm 16)$ MeV. The largest values for the decay width that we were able to obtain within our model are for the case when Z is as small as possible, $Z = 1.47$, and $m_1 = 0$, i.e., when the ρ mass is solely generated by the quark condensate. As seen above, for this case the scattering lengths allow a maximum value $m_\sigma = 477$ MeV, for which $\Gamma_{\sigma\to\pi\pi} \cong 145$ MeV. In all other cases, the decay width is even smaller. However, as will be discussed in Sec. IV A 3, the case $m_1 = 0$ leads to the unphysically small value $\Gamma_{a_1\to\sigma\pi} \simeq 0$ and should therefore not be taken too seriously. As apparent from Fig. 2, excluding small values of m_1 would require smaller values for m_σ in order to be consistent with the scattering lengths. According to Fig. 3, however, this in turn leads to even smaller values for the decay width.

Hence, we conclude that the isoscalar meson in our model cannot be $f_0(600)$, thus excluding that this resonance is predominantly a $\bar{q}q$ state and the chiral partner of the pion. Then the interpretation of the isospin-one state $a_0(980)$ as a (predominantly) quarkonium state is also excluded. The only choice is to consider Scenario II, see Sec. IV B, i.e., to interpret the scalar states above 1 GeV, $f_0(1370)$ and $a_0(1450)$, as being predominantly quarkonia. If the decay width of $f_0(1370)$ can be described by the model, this would be a very strong indication that these higher-lying states can be indeed interpreted as (predominantly) $\bar{q}q$ states. Note that very similar results about the nature of the light scalar mesons were also found using different approaches: from an analysis of the meson behavior in the large-N_c limit in Refs. [31,46] as well as from lattice studies, such as those in Ref. [47].

We remark that the cause for preventing a reasonable fit of the light sigma decay width is the interference term arising from the vector mesons in Eq. (38). In the unphysical case without vector-meson degrees of freedom, a simultaneous fit of the decay width and the scattering lengths is possible [39].

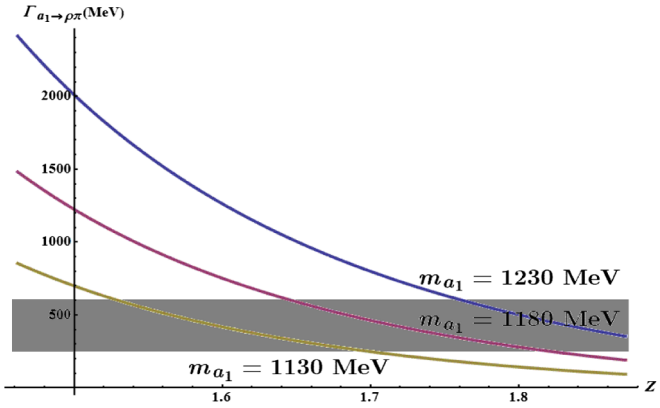

FIG. 4 (color online). $\Gamma_{a_1\to\rho\pi}$ for different values of m_{a_1}. The shaded area corresponds to the possible values of $\Gamma_{a_1\to\rho\pi}$ as stated by the PDG.

3. Decays of the a_1 meson

We first consider the decay width $\Gamma_{a_1\to\rho\pi}$. For a given m_{a_1}, this decay width depends only on Z. The PDG quotes a rather large band of values, $\Gamma^{(\mathrm{exp})}_{a_1\to\rho\pi} = (250\text{–}600)$ MeV. For $m_{a_1} = 1230$ MeV, our fit of meson properties yields $Z = 1.67 \pm 0.2$. The ensuing region is shown as shaded area in Fig. 4. For $m_{a_1} = 1230$ MeV, $\Gamma_{a_1\to\rho\pi}$ decreases from 2.4 GeV to 353 MeV, if Z varies from 1.47 to 1.87.

We also observe from Fig. 4 that the range of values for Z, which give values for $\Gamma_{a_1\to\rho\pi}$ consistent with the experimental error band, becomes larger if one considers smaller masses for the a_1 meson. We have taken $m_{a_1} = 1180$ MeV and $m_{a_1} = 1130$ MeV, the latter being similar to the values used in Refs. [12,48]. Repeating our calculations, we obtain a new range of possible values for Z, $Z \simeq 1.69 \pm 0.2$ for $m_{a_1} = 1180$ MeV and $Z \simeq 1.71 \pm 0.2$ for $m_{a_1} = 1130$ MeV. For the respective central values of Z we then compute $\Gamma^{m_{a_1}=1180\ \mathrm{MeV}}_{a_1\to\rho\pi} = 483$ MeV ($Z^{m_{a_1}=1180\ \mathrm{MeV}} = 1.69$) and $\Gamma^{m_{a_1}=1130\ \mathrm{MeV}}_{a_1\to\rho\pi} = 226$ MeV ($Z^{m_{a_1}=1130\ \mathrm{MeV}} = 1.71$), in good agreement with experimental data. All other results remain valid when m_{a_1} is decreased by about 100 MeV. Most notably, the $f_0(600)$ decay width remains too small.

We also consider the $a_1 \to \sigma\pi$ decay width. Experimental data on this decay channel [21] are inconclusive. The value $\Gamma_{a_1\to\sigma\pi} = 56$ MeV is obtained for the central values of Z, m_1, m_σ, and $\Gamma_{f_1\to a_0\pi}$ (which was used to constrain h_2 via Z). Taking the limit $m_1 = 0$ pulls the value of $\Gamma_{a_1\to\sigma\pi}$ down to practically zero, regardless whether $Z = Z_{\mathrm{min}}$ or $Z = Z_{\mathrm{max}}$. This is an indication that the $m_1 = 0$ limit, where m_ρ is completely generated from the quark condensate, cannot be physical. Note that the case $Z = Z_{\mathrm{max}} = 1.87$ and $m_1 \equiv m_\rho$, i.e., where the quark condensate contribution to the ρ mass vanishes, leads to a rather large value of $\Gamma_{a_1\to\sigma\pi}$, e.g., for the central value of $m_\sigma = 332$ MeV the value of $\Gamma_{a_1\to\sigma\pi} = 120$ MeV follows. Interestingly, this picture persists even if lower values of m_{a_1} are considered. Improving experimental data for this decay channel would allow us to further constrain our parameters.

4. The case of isospin-exact scattering lengths

So far, the values of the scattering lengths used in our fit, $a^0_0 = 0.218 \pm 0.020$ and $a^2_0 = -0.0457 \pm 0.0125$ [41], account for the small explicit breaking of isospin symmetry due to the difference of the up and down quark masses. However, in our model the isospin symmetry is exact. Thus, one should rather use the isospin-exact values $a^{0(\mathrm{I})}_0 = 0.244 \pm 0.020$ and $a^{2(\mathrm{I})}_0 = -0.0385 \pm 0.0125$ [49]. In this section we will briefly show that the conclusions reached so far remain qualitatively unchanged if the isospin-exact values for the scattering lengths are considered.

Performing the χ^2 fit, Eq. (45), with $\Gamma_{a_1\to\pi\gamma}$, $a^{0(\mathrm{I})}_0$ and $a^{2(\mathrm{I})}_0$ as experimental input yields $Z = 1.67 \pm 0.2$—unchanged in comparison with the previous case (Z is largely determined by $\Gamma_{a_1\to\pi\gamma}$ which is the same in both χ^2 calculations), $h_1 = -116 \pm 70$, and $m_\sigma = (284 \pm 16)$ MeV. Note that in this case the errors are much smaller than previously. The reason is that the mean value of m_σ is almost on top of the two-pion decay threshold and thus leads to an artificially small error band. For such small values of m_σ the decay width $\Gamma_{\sigma\to\pi\pi}$ is at least an order of magnitude smaller than the physical value, but even for values of m_σ up to 500 MeV (not supported by our error analysis) the decay width never exceeds 150 MeV, see Fig. 3.

B. Scenario II: Scalar quarkonia above 1 GeV

1. General discussion

A possible way to resolve the problem of the unphysically small two-pion decay width of the sigma meson is to identify the fields σ and a_0 of the model with the resonances $f_0(1370)$ and $a_0(1450)$, respectively. Thus, the scalar quarkonium states are assigned to the energy region above 1 GeV. In the following we investigate the consequences of this assignment. However, the analysis cannot be conclusive for various reasons:

(i) The glueball field is missing. Many studies find that its role in the mass region at about 1.5 GeV is crucial, since it mixes with the other scalar resonances.

(ii) The light scalar mesons below 1 GeV, such as $f_0(600)$ and $a_0(980)$, are not included as elementary fields in our model. The question is if they can be dynamically generated from the pseudoscalar fields already present in our model by solving a Bethe-Salpeter equation. If not, they should be introduced as additional elementary fields from the very beginning (see also the discussion in Ref. [14]).

(iii) Because of absence of the resonance $f_0(600)$, the $\pi\pi$ scattering length a^0_0 cannot be correctly de-

scribed at tree-level: whereas a_0^2 stays always within the experimental error band, a_0^0 clearly requires a light scalar meson for a proper description of experimental data because a large value of m_σ drives this quantity to the Weinberg limit ($\simeq 0.159$) which is outside the experimental error band.

Despite these drawbacks, we turn to a quantitative analysis of this scenario.

2. Decay of the $a_0(1450)$ meson

As in Scenario I, the parameter g_2 can be expressed as a function of Z by using the $\rho \to \pi\pi$ decay width (28). However, the parameter h_2 can no longer be fixed by the $f_1 \to a_0\pi$ decay width: the a_0 meson is now identified with the $a_0(1450)$ resonance listed in Ref. [21], with a central mass of $m_{a_0} = 1474$ MeV, and thus f_1 is too light to decay into a_0 and π. One would be able to determine h_2 from the (energetically allowed) decay $a_0(1450) \to f_1\pi$, but the corresponding decay width is not experimentally known.

Instead of performing a global fit, it is more convenient to proceed step by step and calculate the parameters Z, h_1, h_2 explicitly. We vary $m_\sigma \equiv m_{f_0(1370)}$ within the experimentally known error band [21] and check if our result for $\Gamma_{f_0(1370)\to\pi\pi}$ is in agreement with experimental data.

We first determine Z from $a_1 \to \pi\gamma$, Eq. (37), and obtain $Z = 1.67 \pm 0.21$. We then immediately conclude that the $a_1 \to \rho\pi$ decay width, Eq. (40), will remain the same as in Scenario I because this decay width depends on Z (which is virtually the same in both scenarios) and g_2 [which is fixed via $\Gamma_{\rho\to\pi\pi}$, Eq. (29), in both scenarios].

The parameter h_1, being large-N_c suppressed, will be set to zero in the present study. We then only have to determine the parameter h_2. This is done by fitting the total decay width of the $a_0(1450)$ meson to its experimental value [21],

$$\begin{aligned}\Gamma_{a_0(1450)}(Z, h_2) &= \Gamma_{a_0\to\pi\eta} + \Gamma_{a_0\to\pi\eta'} + \Gamma_{a_0\to KK} \\ &\quad + \Gamma_{a_0\to\omega\pi\pi} \\ &\equiv \Gamma^{(\mathrm{exp})}_{a_0(1450)} = (265 \pm 13)\ \mathrm{MeV}. \end{aligned} \tag{47}$$

Although kaons have not been included into the calculations, we can easily evaluate the decay into KK by using flavor symmetry

$$\Gamma_{a_0(1450)\to KK}(Z, h_2) = 2\frac{k(m_{a_0}, m_K, m_K)}{8\pi m_{a_0}^2}[A_{a_0KK}(Z, h_2)]^2, \tag{48}$$

$$\begin{aligned}A_{a_0KK}(Z, h_2) = \frac{1}{2Zf_\pi}\Big\{m_{\eta_N}^2 - m_{a_0}^2 + \Big(1 - \frac{1}{Z^2}\Big) \\ \times\Big[1 - \frac{1}{2}\frac{Z^2\phi^2}{m_{a_1}^2}(h_2 - h_3)\Big](m_{a_0}^2 - 2m_K^2)\Big\}. \end{aligned} \tag{49}$$

The remaining, experimentally poorly known decay width $\Gamma_{a_0(1450)\to\omega\pi\pi}$ can be calculated from the sequential decay $a_0 \to \omega\rho \to \omega\pi\pi$. Note that the first decay step requires the ρ to be slightly below its mass-shell, since $m_{a_0} < m_\rho + m_\omega$. We denote the off-shell mass of the ρ meson by x. From the Lagrangian (1) we obtain the following formula for the $a_0 \to \omega\rho$ decay width:

$$\begin{aligned}\Gamma_{a_0(1450)\to\omega\rho}(x) = \frac{k(m_{a_0}, m_\omega, x)}{8\pi m_{a_0}^2}(h_2 + h_3)^2 Z^2 f_\pi^2 \\ \times\Big[3 - \frac{x^2}{m_\rho^2} + \frac{(m_{a_0}^2 - x^2 - m_\omega^2)^2}{4m_\omega^2 m_\rho^2}\Big]. \end{aligned} \tag{50}$$

The full decay width $\Gamma_{a_0(1450)\to\omega\pi\pi}$ is then obtained from the following equation:

$$\Gamma_{a_0(1450)\to\omega\pi\pi} = \int_0^\infty dx \Gamma_{a_0\to\omega\rho}(x) d_\rho(x), \tag{51}$$

where $d_\rho(x)$ is the mass distribution of the ρ meson, which is taken to be of relativistic Breit-Wigner form:

$$d_\rho(x) = N\frac{x^2\Gamma^{(\mathrm{exp})}_{\rho\to\pi\pi}}{(x^2 - m_\rho^2)^2 + (x\Gamma^{(\mathrm{exp})}_{\rho\to\pi\pi})^2}\theta(x - 2m_\pi), \tag{52}$$

where $\Gamma^{(\mathrm{exp})}_{\rho\to\pi\pi} = 149.1$ MeV and $m_\rho = 775.49$ MeV [21]. (In general, one should use the theoretical quantity $\Gamma_{\rho\to\pi\pi}$, which is itself a function of x, instead of $\Gamma^{(\mathrm{exp})}_{\rho\to\pi\pi}$, see for instance Refs. [50,51] and references therein. This is, however, numerically irrelevant in the following.) The normalization constant N is chosen such that

$$\int_0^\infty dx d_\rho(x) = 1, \tag{53}$$

in agreement with the interpretation of $dx d_\rho(x)$ as the probability that the off-shell ρ meson has a mass between x and $x + dx$.

Inserting Eqs. (34), (36), (48), and (51) into Eq. (47), we can express h_2 as a function of Z, analogously to Eq. (29) where g_2 was expressed as a function of Z. Similar to that case, we obtain two bands for h_2, $-115 \le h_2 \le -20$ and $-25 \le h_2 \le 10$, the width of the bands corresponding to the uncertainty in determining Z, $Z = 1.67 \pm 0.21$. Both bands for h_2 remain practically unchanged if the 5% experimental uncertainty of $\Gamma^{(\mathrm{exp})}_{a_0(1450)}$ is taken into account and thus we only use the mean value 265 MeV in the following. Since h_1 is assumed to be zero, Eq. (26) allows to express m_1 as a function of Z, $m_1 = m_1(Z, h_1 = 0, h_2(Z))$ (we neglect the experimental uncertainties of m_ρ, m_{a_1}, and f_π). The result is shown in Fig. 5. The first band of (lower) h_2 values should be discarded because it leads to $m_1 > m_\rho$. The second set of (higher) values leads to $m_1 < m_\rho$ only if the lower boundary for Z is 1.60 rather than 1.46. Thus, we shall use the set of larger h_2 values and take the constraint $m_1 < m_\rho$ into account by restricting the

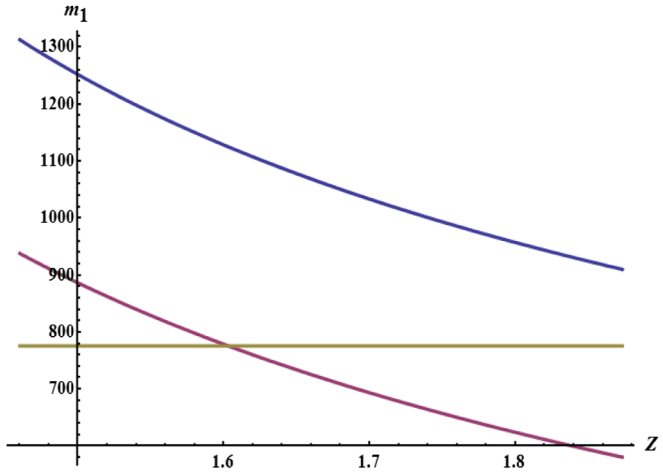

FIG. 5 (color online). Dependence of m_1 on Z. The upper curve corresponds to the lower set of h_2 values and the lower curve to the higher set of h_2 values. The horizontal line corresponds to m_ρ.

values for Z to the range $Z = 1.67^{+0.21}_{-0.07}$. As can be seen from Fig. 5, this sets a lower boundary for the value of m_1, $m_1 \geq 580$ MeV. Thus, in this scenario we obtain $m_1 = 720^{+55}_{-140}$ MeV.

The values for the other parameters can be found in Table II (only central values are shown with the exception of m_1 where the corresponding uncertainties are stated as well).

Note that $\lambda_1 \ll \lambda_2$, in agreement with the expectations from the large-N_c limit, Eq. (19). The value of $m_1 = 720$ MeV is sizable and constitutes a dominant contribution to the ρ mass. This implies that nonquark contributions, for instance a gluon condensate, play a decisive role in the ρ mass generation.

As a final step, we study the ratios $\Gamma_{a_0(1450)\to\eta'\pi}/\Gamma_{a_0(1450)\to\eta\pi}$ and $\Gamma_{a_0(1450)\to K\bar{K}}/\Gamma_{a_0(1450)\to\eta\pi}$. Their experimental values read [21]

$$\frac{\Gamma^{(\mathrm{exp})}_{a_0(1450)\to\eta'\pi}}{\Gamma^{(\mathrm{exp})}_{a_0(1450)\to\eta\pi}} = 0.35 \pm 0.16; \qquad \frac{\Gamma^{(\mathrm{exp})}_{a_0(1450)\to K\bar{K}}}{\Gamma^{(\mathrm{exp})}_{a_0(1450)\to\eta\pi}} = 0.88 \pm 0.23. \tag{54}$$

TABLE II. Central values of the parameters for Scenario II.

Parameter	h_1	h_2	h_3	g_1
Value	0	4.7	2.4	6.4
Parameter	g_2	m_0^2	m_1	λ_1
Value	3.1	$-811\,987$ MeV^2	720^{+55}_{-140} MeV	-3.6
Parameter	λ_2	c	h_0	
Value	84	88 747 MeV^2	1×10^6 MeV^3	

Using the central value $Z = 1.67$ and $\varphi = -36°$ for the η-η' mixing angle, we obtain $\Gamma_{a_0(1450)\to\eta'\pi}/\Gamma_{a_0(1450)\to\eta\pi} = 1.0$ and $\Gamma_{a_0(1450)\to K\bar{K}}/\Gamma_{a_0(1450)\to\eta\pi} = 0.96$. The latter is in very good agreement with the experiment, the former a factor of 2 larger. Note, however, that according to Eqs. (32) and (35) the value of the ratio $\Gamma_{a_0(1450)\to\eta'\pi}/\Gamma_{a_0(1450)\to\eta\pi}$ is proportional to $\sin^2\varphi/\cos^2\varphi$. If a lower value of the angle is considered, e.g., $\varphi = -30°$, then we obtain $\Gamma_{a_0(1450)\to\eta'\pi}/\Gamma_{a_0(1450)\to\eta\pi} = 0.58$ for the central value of Z and the central value of $\Gamma_{a_0(1450)}$ in Eq. (47). Taking $Z = Z_{\max}$ and the upper boundary $\Gamma^{(\mathrm{exp})}_{a_0(1450)} = 278$ MeV results in $\Gamma_{a_0(1450)\to\eta'\pi}/\Gamma_{a_0(1450)\to\eta\pi} = 0.48$, i.e., in agreement with the experimental value. Therefore, our results in this scenario favor a smaller value of φ than the one suggested by the KLOE Collaboration [37].

It is possible to calculate the decay width $\Gamma_{a_0(1450)\to\omega\pi\pi}$ using Eq. (51). We have obtained a very small value $\Gamma_{a_0(1450)\to\omega\pi\pi} = 0.1$ MeV. From Eq. (34) we obtain $\Gamma_{a_0(1450)\to\eta\pi} = 89.5$ MeV, such that the ratio $\Gamma_{a_0(1450)\to\omega\pi\pi}/\Gamma_{a_0(1450)\to\eta\pi} = 0.0012$, in contrast to the results of Ref. [52].

3. Decay of the $f_0(1370)$ meson

It is now possible to calculate the width for the $f_0(1370) \to \pi\pi$ decay using Eq. (38). The decay width depends on the $f_0(1370)$ mass, Z, h_1, and h_2 which is expressed via Z using Eq. (47). The values of the latter three are listed in Table II. In Fig. 6, we show the decay width as a function of the mass of $f_0(1370)$.

Assuming that the two-pion decay dominates the total decay width, we observe a good agreement with the experimental values if $m_{f_0(1370)} \lesssim 1380$ MeV. Other contributions to the decay width are likely to reduce this upper bound on $m_{f_0(1370)}$ somewhat. Nevertheless, the correspondence with the experiment is a lot better in this scenario where we have identified $f_0(1370)$ rather than $f_0(600)$ as the (predominantly) isoscalar $\bar{q}q$ state. Note that this result

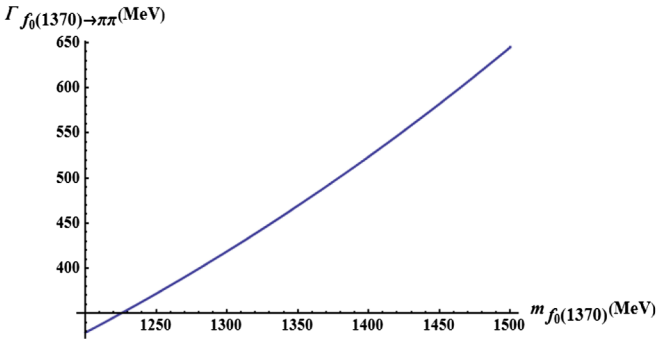

FIG. 6 (color online). Dependence of the $f_0(1370)$ decay width on $m_{f_0(1370)}$. The experimental value of the width is expected to be in the range (1200–1500) MeV [21].

has been obtained using the decay width of the $a_0(1450)$ meson (in order to express h_2 via Z), which is also assumed to be a scalar $\bar{q}q$ state in this scenario.

It is remarkable that vector mesons are crucial to obtain realistic values for the decay width of $f_0(1370)$: without vector mesons, the decay width is ~ 10 GeV and thus much too large. This is why Scenario II has not been considered in the standard linear sigma model.

The four-body decay $f_0(1370) \to 4\pi$ can also be studied. Similarly to the $a_0(1450) \to \omega\rho$ decay, we view $f_0(1370) \to 4\pi$ as a sequential decay of the form $f_0(1370) \to \rho\rho \to 4\pi$. The Lagrangian (1) leads to

$$\Gamma_{f_0(1370)\to\rho\rho}(x_1, x_2) = \frac{3}{16\pi}\frac{k(m_{f_0}, x_1, x_2)}{m_{f_0}^2}(h_1 + h_2 + h_3)^2 Z^2 f_\pi^2 \times \left[4 - \frac{x_1^2 + x_2^2}{m_\rho^2} + \frac{(m_{f_0}^2 - x_1^2 - x_2^2)^2}{4m_\rho^4}\right], \quad (55)$$

where x_1 and x_2 are the off-shell masses of the ρ mesons. The decay width $\Gamma_{f_0\to 4\pi}$ is then given by

$$\Gamma_{f_0(1370)\to 4\pi} = \int_0^\infty \int_0^\infty dx_1 dx_2 \Gamma_{f_0(1370)\to\rho\rho}(x_1, x_2) d_\rho(x_1) \times d_\rho(x_2),$$

with $\Gamma_{f_0(1370)\to\rho\rho}(x_1, x_2)$ from Eq. (55) and $d_\rho(x)$ from Eq. (52).

Using the previous values for the parameters we obtain that the $\rho\rho$ contribution for the decay is small: $\Gamma_{f_0(1370)\to\rho\rho\to 4\pi} \simeq 10 \pm 10$ MeV. (The error comes from varying Z between 1.6 and 1.88.) Reference [53] quotes 54 MeV for the total 4π decay width. Since Ref. [54] ascertains that about 26% of the total 4π decay width originates from the $\rho\rho$ decay channel, our result is consistent with these findings.

V. CONCLUSIONS AND OUTLOOK

We have presented a linear sigma model with vector mesons and global chiral invariance. The motivation for considering global invariance rather than the standard Sakurai model with local chiral invariance (with the exception of the vector-meson mass term) was that the latter fails to describe some important low-energy meson decay processes correctly, most notably the two-pion decay width of the ρ meson [10]. This Lagrangian describes mesons as pure quarkonium states. As shown in Sec. IV A, the resulting low-energy phenomenology is in general in good agreement with experimental data—with one exception: the model fails to correctly describe the $f_0(600) \to \pi\pi$ decay width. This led us to conclude that $f_0(600)$ and $a_0(980)$ cannot be predominantly $\bar{q}q$ states.

Assigning the scalar fields σ and a_0 of the model to the $f_0(1370)$ and $a_0(1450)$ resonances, respectively, improves the results for the decay widths considerably. We have obtained $\Gamma_{f_0(1370)\to\pi\pi} \simeq 300$–$500$ MeV for $m_{f_0(1370)} = 1200$–1400 MeV (see Fig. 6). Thus, the scenario in which the scalar states above 1 GeV, $f_0(1370)$ and $a_0(1450)$, are considered to be (predominantly) $\bar{q}q$ states appears to be favored over the assignment in which $f_0(600)$ and $a_0(980)$ are considered (predominantly) $\bar{q}q$ states. However, a more detailed study of this scenario is necessary, because a glueball state with the same quantum numbers mixes with the quarkonium states. This allows to include the experimentally well-known resonance $f_0(1500)$ into the study.

Of course, interpreting $f_0(1370)$ and $a_0(1450)$ as $\bar{q}q$ states leads to question about the nature of $f_0(600)$ and $a_0(980)$. Their presence is necessary for the correct description of $\pi\pi$ scattering lengths that differ from experiment for too large values of the isoscalar mass (see Sec. IV A 1). We distinguish two possibilities: (i) They can arise as (quasi-)molecular states. This is possible if the attraction in the $\pi\pi$ and KK channels is large enough. In order to prove this, one should solve the corresponding Bethe-Salpeter equation in the framework of Scenario II. In this case $f_0(600)$ and $a_0(980)$ can be classified as genuinely dynamically generated states and should not appear in the Lagrangian, see the discussion in Ref. [14]. If, however, the attraction is not sufficient to generate the two resonances $f_0(600)$ and $a_0(980)$ we are led to the alternative possibility that (ii) these two scalar states must be incorporated into the model as additional tetraquark states. In this case they shall appear from the very beginning in the Lagrangian and should not be considered as dynamically generated states. Of course, the isoscalar tetraquark, quarkonium, and glueball will mix to produce $f_0(600)$, $f_0(1370)$, and $f_0(1500)$, and the isovector tetraquark and quarkonium will mix to produce $a_0(980)$ and $a_0(1450)$.

The issue of restoration of chiral symmetry at nonzero temperature and density is one of the fundamental questions of modern hadron and nuclear physics, see, e.g., Refs. [8,17]. Linear sigma models constitute an effective approach to study chiral symmetry restoration because they contain from the onset not only pseudoscalar and vector mesons, but also their chiral partners with which they become degenerate once the chiral symmetry has been restored. Once vacuum phenomenology is reasonably well reproduced within our model, we also plan to apply it to studies of chiral symmetry restoration at nonzero temperatures and densities.

Another important check of the model is the description of the ALEPH data for the decay of the τ lepton into two and three pions [55]. In this way, we will have a better constraint on the parameters of the model, e.g., the value for the a_1 mass.

An extension of the model to $N_f = 3$ can be performed [56]; with the exception of the strange quark condensate, no further free parameters will arise in this extension.

However, much more data are available for the strange mesons, which constitute an important test for the validity of our approach.

ACKNOWLEDGMENTS

The authors thank J. Schechter, F. Sannino, J. R. Peláez, E. Santini, S. Gallas, and S. Strüber for valuable discussions. The work of D. P. was partially supported by the Foundation "Polytechnical Society." The work of D. P. and F. G. was partially supported by BMBF. The work of D. H. R. was supported by the ExtreMe Matter Institute EMMI. This work was (financially) supported by the Helmholtz International Center for FAIR within the framework of the LOEWE program launched by the State of Hesse.

APPENDIX: THE FULL LAGRANGIAN

This is the final form of the Lagrangian (1) that is obtained after the shifts (9) and the renormalization of the pseudoscalar wave functions; $\rho^{\mu\nu} \equiv \partial^\mu \rho^\nu - \partial^\nu \rho^\mu$; $a_1^{\mu\nu} \equiv \partial^\mu a_1^\nu - \partial^\nu a_1^\mu$; $(\vec{A})_3$ marks the third component of the vector $\vec{A}$. Note that the term $\mathcal{L}_4$ contains the (axial-) vector four-point vertices [the terms $\sim g_{4,5,6,7}$ in the Lagrangian (1)]. We do not give the explicit form of $\mathcal{L}_4$ because it is not relevant for the results that are presented in this paper.

$$
\begin{aligned}
\mathcal{L} = {} & \frac{1}{2}(\partial^\mu \sigma + g_1 Z \vec{\pi}\cdot\vec{a}_1^\mu + g_1 w Z^2 \partial^\mu \vec{\pi}\cdot\vec{\pi} + g_1 Z \eta f_1^\mu + g_1 w Z^2 \eta \partial^\mu \eta)^2 - \frac{1}{2}\left[m_0^2 - c + 3\left(\lambda_1 + \frac{\lambda_2}{2}\right)\phi^2\right]\sigma^2 \\
& + \frac{1}{2}(Z\partial^\mu \vec{\pi} + g_1 Z \vec{\rho}^\mu \times \vec{\pi} - g_1 f_1^\mu \vec{a}_0 - g_1 w Z \partial^\mu \eta \vec{a}_0 - g_1 \sigma \vec{a}_1^\mu - g_1 w Z \sigma \partial^\mu \vec{\pi})^2 \\
& + \frac{1}{2}(Z\partial^\mu \eta - g_1 \sigma f_1^\mu - g_1 w Z \sigma \partial^\mu \eta - g_1 \vec{a}_1^\mu \cdot \vec{a}_0 - g_1 w Z \partial^\mu \vec{\pi}\cdot\vec{a}_0)^2 - \frac{1}{2}\left[m_0^2 - c + \left(\lambda_1 + \frac{\lambda_2}{2}\right)\phi^2\right]Z^2\vec{\pi}^2 \\
& - \frac{1}{2}\left[m_0^2 + c + \left(\lambda_1 + \frac{\lambda_2}{2}\right)\phi^2\right]Z^2\eta^2 + \frac{1}{2}[\partial^\mu \vec{a}_0 + g_1 \vec{\rho}^\mu \times \vec{a}_0 + g_1 Z f_1^\mu \vec{\pi} + g_1 w Z^2 \vec{\pi}\partial^\mu \eta \\
& + g_1 Z \eta \vec{a}_1^\mu + g_1 w Z^2 \eta \partial^\mu \vec{\pi}]^2 - \frac{1}{2}\left[m_0^2 + c + \left(\lambda_1 + \frac{3}{2}\lambda_2\right)\phi^2\right]\vec{a}_0^2 \\
& - \frac{\lambda_2}{2}[(\sigma\vec{a}_0 + Z^2\eta\vec{\pi})^2 + Z^2\vec{a}_0^2\vec{\pi}^2 - Z^2(\vec{a}_0\cdot\vec{\pi})^2] - \frac{1}{4}\left(\lambda_1 + \frac{\lambda_2}{2}\right)(\sigma^2 + \vec{a}_0^2 + Z^2\eta^2 + Z^2\vec{\pi}^2)^2 \\
& - \left(\lambda_1 + \frac{\lambda_2}{2}\right)\phi\sigma(\sigma^2 + \vec{a}_0^2 + Z^2\eta^2 + Z^2\vec{\pi}^2) - \lambda_2\phi\vec{a}_0\cdot(\sigma\vec{a}_0 + Z^2\eta\vec{\pi}) - \frac{1}{4}(\partial^\mu\omega^\nu - \partial^\nu\omega^\mu)^2 + \frac{m_1^2}{2}(\omega^\mu)^2 \\
& - \frac{1}{4}[\partial^\mu\vec{\rho}^\nu - \partial^\nu\vec{\rho}^\mu + g_2\vec{\rho}^\mu\times\vec{\rho}^\nu + g_2\vec{a}_1^\mu\times\vec{a}_1^\nu + g_2 w Z\partial^\mu\vec{\pi}\times\vec{a}_1^\nu + g_2 w Z\vec{a}_1^\mu\times\partial^\nu\vec{\pi} + g_2 w^2 Z^2(\partial^\mu\vec{\pi})\times(\partial^\nu\vec{\pi})]^2
\end{aligned}
$$

$$
\begin{aligned}
& + \frac{m_1^2}{2}(\vec{\rho}^\mu)^2 - \frac{1}{4}(\partial^\mu f_1^\nu - \partial^\nu f_1^\mu)^2 + \frac{m_1^2 + g_1^2\phi^2}{2}(f_1^\mu)^2 + \frac{m_1^2 + g_1^2\phi^2}{2}(\vec{a}_1^\mu)^2 \\
& - \frac{1}{4}[\partial^\mu\vec{a}_1^\nu - \partial^\nu\vec{a}_1^\mu + g_2\vec{\rho}^\mu\times\vec{a}_1^\nu + g_2 w Z\vec{\rho}^\mu\times\partial^\nu\vec{\pi} + g_2\vec{a}_1^\mu\times\vec{\rho}^\nu + g_2 w Z(\partial^\mu\vec{\pi})\times\vec{\rho}^\nu]^2 \\
& - g_1^2\phi\vec{a}_{1\mu}\cdot[\vec{\rho}^\mu\times Z\vec{\pi} - f_1^\mu\vec{a}_0 - wZ\vec{a}_0\partial^\mu\eta] - g_1^2 wZ\phi\partial_\mu\vec{\pi}\cdot[Z\vec{\rho}^\mu\times\vec{\pi} - f_1^\mu\vec{a}_0 - wZ\partial^\mu\eta\vec{a}_0] \\
& + g_1^2\phi f_{1\mu}(\vec{a}_1^\mu\cdot\vec{a}_0 + wZ\partial^\mu\vec{\pi}\cdot\vec{a}_0) + g_1^2 wZ\phi\partial_\mu\eta(\vec{a}_1^\mu\cdot\vec{a}_0 + wZ\partial^\mu\vec{\pi}\cdot\vec{a}_0) \\
& + g_1^2\phi\sigma[(f_1^\mu)^2 + 2wZf_{1\mu}\partial^\mu\eta + w^2Z^2(\partial^\mu\eta)^2] \\
& + g_1^2\phi\sigma[(\vec{a}_1^\mu)^2 + 2wZ\vec{a}_{1\mu}\cdot\partial^\mu\vec{\pi} + w^2Z^2(\partial^\mu\vec{\pi})^2] - \frac{1}{2}\frac{g_1^2\phi^2}{m_{a_1}^2}Z^2(\partial_\mu\eta\partial^\mu\eta + \partial_\mu\vec{\pi}\cdot\partial^\mu\vec{\pi})
\end{aligned}
$$

$$
\begin{aligned}
&+ eA_\mu\{(\vec{a}_0 \times \partial^\mu \vec{a}_0)_3 + Z^2(\vec{\pi} \times \partial^\mu \vec{\pi})_3 - 4(\vec{\rho}^{\mu\nu} \times \vec{\rho}_\nu)_3 - 4[(\vec{a}_{1\nu} + Zw\partial_\nu \vec{\pi}) \times \vec{a}_1^{\mu\nu}]_3 \\
&+ g_1\{2Z(f_1^\mu + Zw\partial^\mu \eta)(\vec{a}_0 \times \vec{\pi})_3 + Z(\sigma + \phi)[(\vec{a}_1^\mu + Zw\partial^\mu \vec{\pi}) \times \vec{\pi}]_3 + \eta[\vec{a}_0 \times (\vec{a}_1^\mu + Zw\partial^\mu \vec{\pi})]_3 \\
&- a_0^3(a_0^1\rho^{\mu 1} + a_0^2\rho^{\mu 2}) - Z^2\pi^3(\pi^1\rho^{\mu 1} + \pi^2\rho^{\mu 2}) + \rho^{\mu 3}[(a_0^1)^2 + (a_0^2)^2 + Z^2(\pi^1)^2 + Z^2(\pi^2)^2]\} \\
&+ 4g_2\{[\vec{\rho}_\nu^2 + \vec{a}_{1\nu}^2 + Z^2w^2(\partial_\nu \vec{\pi})^2 + Zw\vec{a}_{1\nu} \cdot \partial^\nu \vec{\pi}]\rho^{\mu 3} + 2\vec{\rho}_\nu \cdot (\vec{a}_1^\nu + Zw\partial^\nu \vec{\pi}) \times (a_1^{\mu 3} + Zw\partial^\mu \pi^3) \\
&- (\vec{\rho}_\nu \cdot \vec{\rho}^\mu + \vec{a}_{1\nu} \cdot \vec{a}_1^\mu + Zw\vec{a}_{1\nu} \cdot \partial^\mu \vec{\pi} + Zw\vec{a}_1^\mu \cdot \partial_\nu \vec{\pi} + Z^2w^2\partial_\nu \vec{\pi} \cdot \partial^\mu \vec{\pi})\rho^{\nu 3} \\
&- (\vec{\rho}^\mu \cdot \vec{a}_{1\nu} + \vec{a}_1^\mu \cdot \vec{\rho}_\nu + Zw\vec{\rho}^\mu \cdot \partial_\nu \vec{\pi} + Zw\vec{\rho}_\nu \cdot \partial^\mu \vec{\pi})a_1^{\nu 3}\}\} + \frac{e^2}{2}A_\mu A^\mu[(a_0^1)^2 + (a_0^2)^2 + Z^2(\pi^1)^2 \\
&+ Z^2(\pi^2)^2 + 4(\rho^{\nu 1})^2 + 4(\rho^{\nu 2})^2 + 4(a_{1\nu}^1 + Zw\partial_\nu \pi^1)^2 + 4(a_{1\nu}^2 + Zw\partial_\nu \pi^2)^2] \\
&- 2e^2A_\mu A_\nu[\rho^{\mu 1}\rho^{\nu 1} + \rho^{\mu 2}\rho^{\nu 2} + (a_1^{\mu 1} + Zw\partial^\mu \pi^1)(a_1^{\nu 1} + Zw\partial^\nu \pi^1) + (a_1^{\mu 2} + Zw\partial^\mu \pi^2)(a_1^{\nu 2} + Zw\partial^\nu \pi^2)] \\
&+ \mathcal{L}_{h_{1,2,3}} + \mathcal{L}_{g_3} + \mathcal{L}_4
\end{aligned}
$$

$$
\begin{aligned}
\mathcal{L}_{h_{1,2,3}} = &\left(\frac{h_1}{4} + \frac{h_2}{4} + \frac{h_3}{4}\right)(\sigma^2 + 2\phi\sigma + Z^2\eta^2 + \vec{a}_0^2 + Z^2\vec{\pi}^2)(\omega_\mu^2 + \vec{\rho}_\mu^2) + \left(\frac{h_1}{4} + \frac{h_2}{4} - \frac{h_3}{4}\right) \\
&\times (\sigma^2 + 2\phi\sigma + Z^2\eta^2 + \vec{a}_0^2 + Z^2\vec{\pi}^2)\{f_{1\mu}^2 + \vec{a}_{1\mu}^2 + Z^2w^2[(\partial_\mu \eta)^2 + (\partial_\mu \vec{\pi})^2] + 2Zw(f_{1\mu}\partial^\mu \eta + \vec{a}_{1\mu} \cdot \partial^\mu \vec{\pi})\} \\
&+ \left(\frac{h_1}{4} + \frac{h_2}{4} + \frac{h_3}{4}\right)\phi^2(\omega_\mu^2 + \vec{\rho}_\mu^2) + \left(\frac{h_1}{4} + \frac{h_2}{4} - \frac{h_3}{4}\right)\phi^2(f_{1\mu}^2 + \vec{a}_{1\mu}^2) + (h_2 + h_3)\omega_\mu[(\sigma + \phi)\vec{a}_0 + Z^2\eta\vec{\pi}] \cdot \vec{\rho}^\mu \\
&+ (h_2 - h_3)[(\sigma + \phi)\vec{a}_0 + Z^2\eta\vec{\pi}] \cdot [f_{1\mu}\vec{a}_1^\mu + Zw(\vec{a}_{1\mu}\partial^\mu \eta + f_{1\mu}\partial^\mu \vec{\pi}) + Z^2w^2(\partial_\mu \eta)(\partial^\mu \vec{\pi})] \\
&+ (h_2 + h_3)Z(\vec{a}_0 \times \vec{\pi}) \cdot (\omega_\mu \vec{a}_1^\mu + Zw\omega_\mu \partial^\mu \vec{\pi}) + (h_2 - h_3)Z(\vec{a}_0 \times \vec{\pi}) \cdot (f_{1\mu}\vec{\rho}^\mu + Zw\vec{\rho}_\mu \partial^\mu \eta) \\
&+ h_3Z[\eta\vec{a}_0 - (\sigma + \phi)\vec{\pi}] \cdot [\vec{\rho}_\mu \times (\vec{a}_1^\mu + Zw\partial^\mu \vec{\pi})] - \frac{h_3}{2}\{(\vec{a}_0 \times \vec{\rho}^\mu)^2 - [\vec{a}_0 \times (\vec{a}_1^\mu + Zw\partial^\mu \vec{\pi})]^2 \\
&+ Z^2(\vec{\pi} \times \vec{\rho}^\mu)^2 - Z^2[\vec{\pi} \times (\vec{a}_1^\mu + Zw\partial^\mu \vec{\pi})]^2\}
\end{aligned}
$$

$$
\begin{aligned}
\mathcal{L}_{g_3} = &-4g_3\{\partial_\mu \omega_\nu[\omega^\mu\omega^\nu + f_1^\mu f_1^\nu + \vec{\rho}^\mu \cdot \vec{\rho}^\nu + \vec{a}_1^\mu \cdot \vec{a}_1^\nu + Zw(f_1^\mu \partial^\nu \eta + f_1^\nu \partial^\mu \eta + \vec{a}_1^\mu \cdot \partial^\nu \vec{\pi} + \vec{a}_1^\nu \cdot \partial^\mu \vec{\pi}) \\
&+ Z^2w^2(\partial^\mu \eta\partial^\nu \eta + \partial^\mu \vec{\pi} \cdot \partial^\nu \vec{\pi})] + (\partial_\mu f_{1\nu} + Zw\partial_\mu \partial_\nu \eta)[\omega^\mu f_1^\nu + \omega^\nu f_1^\mu + \vec{\rho}^\mu \cdot \vec{a}_1^\nu + \vec{\rho}^\nu \cdot \vec{a}_1^\mu \\
&+ Zw(\omega^\mu \partial^\nu \eta + \omega^\nu \partial^\mu \eta + \vec{\rho}^\mu \cdot \partial^\nu \vec{\pi} + \vec{\rho}^\nu \cdot \partial^\mu \vec{\pi})] + \partial_\mu \vec{\rho}_\nu \cdot [\omega^\mu \vec{\rho}^\nu + \omega^\nu \vec{\rho}^\mu + f_1^\mu \vec{a}_1^\nu + f_1^\nu \vec{a}_1^\mu \\
&+ Zw(\vec{a}_1^\mu \partial^\nu \eta + \vec{a}_1^\nu \partial^\mu \eta + f_1^\mu \partial^\nu \vec{\pi} + f_1^\nu \partial^\mu \vec{\pi}) + Z^2w^2(\partial^\mu \eta\partial^\nu \vec{\pi} + \partial^\nu \eta\partial^\mu \vec{\pi})] + (\partial_\mu \vec{a}_{1\nu} + Zw\partial_\mu \partial_\nu \vec{\pi}) \\
&\cdot [f_1^\mu \vec{\rho}^\nu + f_1^\nu \vec{\rho}^\mu + \omega^\mu \vec{a}_1^\nu + \omega^\nu \vec{a}_1^\mu + Zw(\vec{\rho}^\mu \partial^\nu \eta + \vec{\rho}^\nu \partial^\mu \eta + \omega^\mu \partial^\nu \vec{\pi} + \omega^\nu \partial^\mu \vec{\pi})]\} \\
&+ 4eg_3A_\mu\{\omega_\nu[(\vec{\rho}^\mu \times \vec{\rho}^\nu)_3 + (\vec{a}_1^\mu \times \vec{a}_1^\nu)_3 + Zw(\partial^\mu \vec{\pi} \times \vec{a}_1^\nu)_3 + Zw(\vec{a}_1^\mu \times \partial^\nu \vec{\pi})_3 + Z^2w^2(\partial^\mu \vec{\pi} \times \partial^\nu \vec{\pi})_3] \\
&+ (f_{1\nu} + Zw\partial_\nu \eta)[(\vec{\rho}^\mu \times \vec{a}_1^\nu)_3 + (\vec{a}_1^\mu \times \vec{\rho}^\nu)_3 + Zw(\vec{\rho}^\mu \times \partial^\nu \vec{\pi})_3 + Zw(\partial^\mu \vec{\pi} \times \vec{\rho}^\nu)_3]\}
\end{aligned}
$$

[1] J. S. Schwinger, Ann. Phys. (N.Y.) **2**, 407 (1957); M. Gell-Mann and M. Levy, Nuovo Cimento **16**, 705 (1960); S. Weinberg, Phys. Rev. Lett. **18**, 188 (1967).
[2] J. S. Schwinger, Phys. Lett. B **24**, 473 (1967); S. Weinberg, Phys. Rev. **166**, 1568 (1968).
[3] G. 't Hooft, Phys. Rep. **142**, 357 (1986).
[4] R. D. Peccei, Lect. Notes Phys. **741**, 3 (2008).
[5] C. Vafa and E. Witten, Nucl. Phys. **B234**, 173 (1984); L. Giusti and S. Necco, J. High Energy Phys. 04 (2007) 090.
[6] S. Gasiorowicz and D. A. Geffen, Rev. Mod. Phys. **41**, 531 (1969).
[7] P. Ko and S. Rudaz, Phys. Rev. D **50**, 6877 (1994).
[8] S. Strüber and D. H. Rischke, Phys. Rev. D **77**, 085004 (2008).
[9] U. G. Meissner, Phys. Rep. **161**, 213 (1988).
[10] D. Parganlija, F. Giacosa, and D. H. Rischke, AIP Conf. Proc. **1030**, 160 (2008).
[11] D. Parganlija, F. Giacosa, and D. H. Rischke, Proc. Sci., CONFINEMENT8 (2008) 070.
[12] M. Urban, M. Buballa, and J. Wambach, Nucl. Phys. **A697**, 338 (2002).
[13] S. Gallas, F. Giacosa, and D. H. Rischke, Phys. Rev. D **82**, 014004 (2010).
[14] F. Giacosa, Phys. Rev. D **80**, 074028 (2009).

[15] C. Amsler and F. E. Close, Phys. Lett. B **353**, 385 (1995); W. J. Lee and D. Weingarten, Phys. Rev. D **61**, 014015 (1999); F. E. Close and A. Kirk, Eur. Phys. J. C **21**, 531 (2001); F. Giacosa, T. Gutsche, V. E. Lyubovitskij, and A. Faessler, Phys. Rev. D **72**, 094006 (2005); Phys. Lett. B **622**, 277 (2005).

[16] R. L. Jaffe, Phys. Rev. D **15**, 267 (1977); **15**, 281 (1977); L. Maiani, F. Piccinini, A. D. Polosa, and V. Riquer, Phys. Rev. Lett. **93**, 212002 (2004); A. H. Fariborz, R. Jora, and J. Schechter, Phys. Rev. D **72**, 034001 (2005); F. Giacosa, Phys. Rev. D **74**, 014028 (2006); A. H. Fariborz, R. Jora, and J. Schechter, Phys. Rev. D **76**, 114001 (2007); F. Giacosa, Phys. Rev. D **75**, 054007 (2007); G. 't Hooft, G. Isidori, L. Maiani, A. D. Polosa, and V. Riquer, Phys. Lett. B **662**, 424 (2008); T. Kojo and D. Jido, Phys. Rev. D **78**, 114005 (2008); arXiv:0807.2364.

[17] A. Heinz, S. Struber, F. Giacosa, and D. H. Rischke, Phys. Rev. D **79**, 037502 (2009).

[18] G. 't Hooft, Nucl. Phys. **B72**, 461 (1974); E. Witten, Nucl. Phys. **B160**, 57 (1979); S. R. Coleman, in *Pointlike Structures Inside and Outside Hadrons*, edited by A. Zichichi (Plenum Press, New York, 1982), 0011; R. F. Lebed, Czech. J. Phys. **49**, 1273 (1999).

[19] J. Boguta, Phys. Lett. **120B**, 34 (1983); O. Kaymakcalan and J. Schechter, Phys. Rev. D **31**, 1109 (1985); R. D. Pisarski, arXiv:hep-ph/9503330.

[20] S. Gallas, F. Giacosa, and D. H. Rischke, Proc. Sci., CONFINEMENT8 (2008) 089.

[21] C. Amsler *et al.*, (Particle Data Group), Phys. Lett. B **667**, 1 (2008) and 2009 partial update for the 2010 edition.

[22] G. Ecker, J. Gasser, A. Pich, and E. de Rafael, Nucl. Phys. **B321**, 311 (1989); G. Ecker, J. Gasser, H. Leutwyler, A. Pich, and E. de Rafael, Phys. Lett. B **223**, 425 (1989).

[23] M. Bando, T. Kugo, and K. Yamawaki, Phys. Rep. **164**, 217 (1988).

[24] M. C. Birse, Z. Phys. A **355**, 231 (1996).

[25] H. B. O'Connell, B. C. Pearce, A. W. Thomas, and A. G. Williams, Prog. Part. Nucl. Phys. **39**, 201 (1997).

[26] J. J. Sakurai, Ann. Phys. (N.Y.) **11**, 1 (1960).

[27] C. N. Yang and R. L. Mills, Phys. Rev. **96**, 191 (1954).

[28] D. Lurie, *Particles and Fields* (John Wiley & Sons, New York, 1968).

[29] L. Roca, E. Oset, and J. Singh, Phys. Rev. D **72**, 014002 (2005).

[30] L. S. Geng, E. Oset, J. R. Pelaez, and L. Roca, Eur. Phys. J. A **39**, 81 (2009).

[31] J. R. Pelaez, Phys. Rev. Lett. **92**, 102001 (2004); AIP Conf. Proc. **814**, 670 (2006); J. R. Pelaez and G. Rios, Phys. Rev. Lett. **97**, 242002 (2006).

[32] M. Wagner and S. Leupold, Phys. Lett. B **670**, 22 (2008).

[33] S. Schael *et al.* (ALEPH Collaboration), Phys. Rep. **421**, 191 (2005).

[34] M. Harada and K. Yamawaki, Phys. Rep. **381**, 1 (2003).

[35] K. Kawarabayashi and M. Suzuki, Phys. Rev. Lett. **16**, 255 (1966); Riazuddin and Fayyazuddin, Phys. Rev. **147**, 1071 (1966).

[36] F. Giacosa, arXiv:0712.0186.

[37] F. Ambrosino *et al.*, J. High Energy Phys. 07 (2009) 105.

[38] D. V. Bugg, V. V. Anisovich, A. Sarantsev, and B. S. Zou, Phys. Rev. D **50**, 4412 (1994).

[39] D. Parganlija, F. Giacosa, and D. H. Rischke, arXiv:0911.3996.

[40] B. Ananthanarayan, G. Colangelo, J. Gasser, and H. Leutwyler, Phys. Rep. **353**, 207 (2001).

[41] B. Peyaud (NA48 Collaboration), Nucl. Phys. B, Proc. Suppl. **187**, 29 (2009).

[42] A. H. Fariborz, N. W. Park, J. Schechter, and M. Naeem Shahid, Phys. Rev. D **80**, 113001 (2009); A. H. Fariborz, R. Jora, and J. Schechter, Phys. Rev. D **79**, 074014 (2009).

[43] M. S. Bhagwat, L. Chang, Y. X. Liu, C. D. Roberts, and P. C. Tandy, Phys. Rev. C **76**, 045203 (2007).

[44] H. Leutwyler, AIP Conf. Proc. **1030**, 46 (2008).

[45] R. Kaminski, R. Garcia-Martin, P. Grynkiewicz, and J. R. Pelaez, Nucl. Phys. B, Proc. Suppl. **186**, 318 (2009).

[46] M. Harada, F. Sannino, and J. Schechter, Phys. Rev. D **69**, 034005 (2004).

[47] N. Mathur *et al.*, Phys. Rev. D **76**, 114505 (2007); T. Draper, T. Doi, K. F. Liu, D. Mankame, N. Mathur, and X. f. Meng, Proc. Sci., LATTICE2008 (2008) 108.

[48] C. S. Fischer and R. Williams, Phys. Rev. Lett. **103**, 122001 (2009).

[49] B. Bloch-Devaux (NA48/2 Collaboration), Nucl. Phys. **A827**, 234c (2009).

[50] F. Giacosa and G. Pagliara, Phys. Rev. C **76**, 065204 (2007).

[51] E. Santini, M. D. Cozma, A. Faessler, C. Fuchs, M. I. Krivoruchenko, and B. Martemyanov, Phys. Rev. C **78**, 034910 (2008); W. Peters, M. Post, H. Lenske, S. Leupold, and U. Mosel, Nucl. Phys. **A632**, 109 (1998); M. Post, S. Leupold, and U. Mosel, Nucl. Phys. **A689**, 753 (2001).

[52] C. A. Baker *et al.*, Phys. Lett. B **563**, 140 (2003).

[53] D. V. Bugg, Eur. Phys. J. C **52**, 55 (2007).

[54] A. Abele *et al.* (CRYSTAL BARREL Collaboration), Eur. Phys. J. C **21**, 261 (2001).

[55] A. Habersetzer, F. Giacosa, and D. H. Rischke (unpublished).

[56] D. Parganlija, F. Giacosa, and D. H. Rischke (unpublished).